POLITECNICO DI TORINO
Repository ISTITUZIONALE

Thermal transport phenomena in nanoparticle suspensions

(Article begins on next page)

19 April 2024

Thermal transport phenomena in nanoparticle suspensions

Topical review

Annalisa Cardellini, Matteo Fasano, Masoud Bozorg Bigdeli, Eliodoro Chiavazzo, Pietro Asinari

Department of Energy, Politecnico di Torino, Corso Duca degli Abruzzi 24, 10129 Torino, Italy

E-mail: `pietro.asinari@polito.it`

Abstract. Nanoparticle suspensions in liquids have received great attention, as they may offer an approach to enhance thermophysical properties of base fluids. A good variety of applications in engineering and biomedicine has been investigated with the aim of exploiting the above potential. The multiscale nature of nanosuspensions raises several issues in defining a comprehensive modelling framework, incorporating relevant molecular details and much larger scale phenomena, such as particle aggregation and their dynamics. The objectives of the present topical review is to report and discuss the main heat and mass transport phenomena ruling their macroscopic behaviour, arising from molecular details. Relevant experimental results are included and properly put in the context of recent observations and theoretical studies, which solved long-standing debates about thermophysical properties enhancement. Major transport phenomena are discussed and in-depth analysis is carried out for highlighting the role of geometrical (nanoparticle shape, size, aggregation, concentration), chemical (pH, surfactants, functionalization) and physical parameters (temperature, density). We finally overview several computational techniques available at different scales with the aim of drawing the attention on the need for truly multiscale predictive models. This may help the development of next-generation nanoparticle suspensions and their rational use in thermal applications.

1. Introduction

Solid nanoparticles with size less than 100 nm have been adopted to alter the properties of bulk materials for thousands of years: prototypical example is offered by the glittering effect of gold-ruby glass in ancient artifacts [1]. However, the controlled synthesis of nanoparticles was only achieved with the modern advancement in nanotechnology in the 1980s [2]. While first years of nanoparticle research focused on synthesis techniques, later studies shifted the attention to applications, with particular focus on nanoparticle suspension or nanosuspensions in liquids [2, 3]. In fact, suspending

nanoparticles in a liquid may be an effective way of tuning the thermophysical, optical, electromagnetic and chemical properties of the base fluid [4]. In particular, in 1995 Choi and collaborators have first suggested that nanoparticle suspensions may serve as next-generation heat transfer fluids (nanofluids) [5], mostly because of their increased thermal conductivity [6]. However, the multiscale nature of nanosuspensions has always limited a more fundamental derivation of their macroscopic properties from nanoscale characteristics. Therefore, an *a posteriori* modeling and justification of experimental features of nanoparticle suspensions is the general approach found in the literature [2]. Recent research is instead starting to explore multiscale models for *a priori* prediction of nanosuspensions properties; moreover, other fields of application are currently gaining momentum, in addition to the more traditional thermal engineering ones [7, 8].

For example, nanoparticle suspensions find application as magnetic sealants [9], lubricants [10, 11], fluids for enhanced oil recovery [12], dielectric transformer oils [13], photocatalysts [14–16], catalysts [17], fuel additives [18], preparation of antireflective [19] and hydrophobic [20] surfaces. Colloidal dispersions of magnetic nanoparticles [21–23], also referred to as ferrofluids, can take advantage of their response to applied magnetic fields in several applications, including actuators, lubrication, sensors, seals and magnetically driven assembly of structures [24]. Several nanoparticles in aqueous solutions have been found to efficiently convert solar energy to steam [25–27], such as gold by plasmonic effect and graphene by large solar light absorptance. To this respect, volumetric solar receivers based on nanosuspensions have been studied for enhanced solar-to-thermal energy conversion [28–31]. Furthermore, Janus particles with two or more distinct physical properties are recently being investigated in colloids with smart self-assembly capabilities [32]. Nanosuspensions show great potential also in the biomedical sector, especially in nanocryosurgery [33], antibacterial [34], drug delivery [35, 36], diagnostic [37, 38] and therapeutic [39–41] purposes. In particular, gold- or iron oxides-based nanosuspensions are showing promising potential for hyperthermic therapies, where a strong, localized hyperthermia treatment has been demonstrated to be effective against tumors [42].

One of the main features of colloidal nanosuspensions is the very high thermal conductivity of solid nanoparticles, which can be hundreds or thousands of times greater than that of conventional heat transfer fluids. The challenge is to use this feature in order to enhance the mean-field thermal conductivity of the suspension as a whole [3, 5, 7, 43–48]. Early experimental findings suggested that nanofluids containing a limited concentration of dispersed nanoparticles can lead to considerable increase in thermal transfer properties (e.g. 30% thermal conductivity enhancement for TiO_2-water suspensions [49]) respect to those of the base fluids. Moreover, nanofluids show better stability respect to fluids added with micrometer- or millimeter-sized particles, due to Brownian motion of nanoparticles [50, 51]. Therefore, nanofluids have been extensively investigated as novel coolants for electronic [52, 53], nuclear or automotive components [54–58], with the potential to reduce the size of traditional heat exchangers. However, nanoparticles also cause a general increase in fluid viscosity, thus leading to an increased

pumping power and corrosion of mechanical components. As a results, those issues are still limiting a wide commercial exploitation of nanofluids [45, 59–62].

Nanofluids have been the subject of much hype in the last several years, with many claims of exceptional properties implying the existence of new and still un-understood physical processes and the like. More recently, many controversial results have been clarified and well-understood physics restored to the place to which it belongs. It is now quite well understood that the actual heat diffusivity of nanofluids depends on three aspects: the properties of the solid particles and suspending fluid, the interfacial resistance, and most importantly the morphology of the aggregates that form in the suspension [63]. Firstly, nanoscale solid materials are characterized by large thermal conductivities, e.g. 3500 W/mK of carbon nanotubes [64]. Secondly, thermal boundary resistance or Kapitza resistance is observed at solid-liquid interfaces due to phonon scattering [65]. As the size of structures approaches nanometer dimensions, thermal boundary resistance becomes a critical quantity in the heat transfer due to the large density of interfaces [66]. Moreover, temperature, surface chemistry, shape, roughness and functionalization of nanoparticles are observed to affect Kapitza resistance at solid-liquid interface [67–72]. Thirdly, the agglomeration of nanoparticles favorites the creation of percolation paths in the nanosuspension, therefore altering the overall thermal transmittance [73–75]. In general, it can be said that the benefit of nanofluids for heat transfer applications has been largely exaggerated [76], as the presence of aggregates also affects the viscosity. Hence, the future research should address the issue of optimization of nanofluid aggregate morphologies leading to the best combination of thermal conductivity and viscosity [63], still preserving stability and good optical properties.

Other peculiar properties of nanosuspensions are contributing to shift the attention from heat transfer to other applications. For example, both surface wettability and curvature influence the boiling behavior of water in the proximity of nanoparticles [77, 78], and significant increases in critical heat flux in boiling heat transfer have been observed in nanosuspensions [79, 80]. Moreover, a temperature gradient can also work as a driving force for mass diffusion in Brownian mixtures of two or more species (thermophoresis) [81–83]. Furthermore, new perspectives are offered by nanofluids designed with more than one optimized feature. The nanofluids designed for enhancing more than one thermo-physical property, e.g. both thermal conductivity and optical absorption, are called *hybrid nanofluids*. For example, nanosuspensions have the potential to revolutionize the solar thermal sector because nanoparticles (i) can enhance the thermal conductivity and hence the heat transfer efficiency and (ii) can be optically active and therefore used as direct absorbers [8, 30].

Despite the encouraging commercialization of nanosuspensions in some specific applications [84], a widespread industrial adoption of nanoparticle suspensions may be hindered by issues such as long term stability, increased pressure drops, lower specific heat and limited synthesis repeatability [7, 51]. Hence, a more comprehensive understanding of the involved multiscale heat and mass transfer mechanisms is still

needed for a rational design of nanosuspensions. In fact, design parameters such as thermal conductivity and viscosity are function of a large variety of geometrical (nanoparticle shape, size, aggregation, concentration), chemical (pH, surfactants, coating) and physical (temperature, density) characteristics of the nanosuspension [45]. This pronounced sensitivity is the main reason for some contradictory results between experimental evidences and theoretical considerations presented in the literature [79]. Molecular simulations can indeed support experiments to achieve a more profound understanding of the transport properties of nanosuspensions, especially with complex phenomena such as particle aggregation; whereas the development of better synthesis techniques is progressively facilitating more accurate experimental investigations [7].

In this article, the main thermal transport phenomena occurring in nanoparticle suspensions are reviewed. Experimental evidences and current theoretical understanding are first presented. Then, computational tools for investigating transport properties of nanoparticle suspensions at multiple scales are reported. Finally, future directions and perspectives of nanosuspension research are outlined. The present review is intended to offer a wide overview of the main experimental, theoretical and computational tools and evidences to achieve multiscale predictive models for the heat transport properties of nanoparticle suspensions, which may unlock a more systematic transfer from lab-scale tests to industrial commercialization.

2. Experimental investigations

2.1. Synthesis and measurement techniques

Nanosuspensions are made out of solid nanoparticles suspended in a base fluid. Generally, surface active agents (surfactants) are also introduced, in order to improve the stability of the suspension [85]. Based on the thermophysical properties required for the intended application, a suitable particle core, coating and base fluid should be carefully engineered. Typically synthesized nanoparticle core may be metallic (Ag, Al, Au, Cu, Fe), ceramic (AlN, Al_2O_3, CuO, Fe_3O_4, SiC, SiN, SiO_2, TiC, TiO_2, ZnO, ZrO_2) or carbon-based (graphene, fullerene, single- or multi-walled carbon nanotubes) [3, 86, 87]. Nanoparticles can be produced by several physical or chemical synthesis techniques, e.g. mechanical attrition, gas condensation or chemical precipitation [3, 4]. From both quality and economical reasons, gas phase techniques are the most appropriate for large-scale synthesis of nanoparticles [45]. In thermal applications, the base fluids in which nanoparticles are usually suspended are conventional heat transfer fluids (e.g. water, oil, ethylene glycol [62]), whereas other continuous media (e.g. acetone, decene, PBS, liquid gallium or mercury [88, 89]) can be adopted in different applications [4].

Nanosuspensions are typically produced by either two- or one-step techniques [3]. In two-step techniques (top-down approach), dried nanoparticles are first synthesized by physical or chemical process, then directly dispersed into the base fluid. The top-down approach has been extensively adopted in synthesizing nanosuspensions because

of the widespread commercial availability of various nanopowders [90–92], therefore allowing large-scale and economical synthesis [48]. However, two-step techniques are generally unsuitable for suspensions of pure metal nanoparticles, because of possible surface oxidation during the processes of drying, storage, transportation and dispersion of nanoparticles [51]. These intermediate production steps may be also responsible of increased particle aggregation phenomena [48]. On the other hand, in one-step techniques (bottom-up approach) nanoparticles are simultaneously synthesized and dispersed into the base fluid [45, 93, 94]. Therefore, one-step methods prevent surface oxidation and limit nanoparticle aggregation, therefore improving the suspension stability [31, 62]. Nevertheless, the bottom-up approach may leave residual reactants due to incomplete reactions in the nanoparticle suspension, thus altering the resulting properties [45]. Single-step methods are usually characterized by lower productivity and higher production costs [95, 96].

The stability of nanocolloids is given by the long time suspension of nanoparticles in the base fluid. This is usually achieved by avoiding the formation of large particle clusters and agglomerates, thanks to either simple physical (e.g. sonication, high-shear mixing [50, 59]) or chemical dispersion methods. In chemical dispersion methods, electrostatic interaction, steric effect or functional group attachment on the nanoparticles surface are used to limit the interparticle van der Waals forces leading to clustering phenomena [59]. While electrostatic surface charge of nanoparticles can be tuned by pH [44], steric repulsion is obtained by introducing surfactants in the suspension [85]. Surfactants are long organic molecules with both lipophilic and hydrophilic groups, which lower the surface tension between nanoparticles and fluid. Surfactants should be carefully chosen according to the properties of the particles and solution [44]. Surfactants commonly used in nanofluids are SDBS, gum Arabic, chitosan, CTAB, Gemini and Triton X-100 [31, 97, 98]. However, surfactants may significantly alter the heat transfer, optical and visco-elastic properties of nanosuspensions, especially at high temperatures [8, 44, 45]. Beside surfactants, the modification of particle surface properties by chemical functionalization can be also adopted to avoid aggregation [31]. For example, the suspension of hydrophobic particles in water requires chemical functionalization of the particle surface with hydrophilic coating, and vice versa in case of hydrophilic particles suspended in oil [99]. Therefore, the optimal surface properties of nanoparticles can be achieved by modifying (i.e. coating) the nanoparticle core surface with functional layers or stabilizers, which are added during the synthesis.

Several methods have been adopted to measure the main thermal and fluid properties of nanosuspensions. Thermal conductivity is usually measured by steady state or transient methods [47]. Steady state methods include cylindrical cell [100] and steady state parallel plate [101]; whereas hot-wire method [102], temperature oscillation [103], thermal constants analyzer [104] and 3ω method [105] belong to transient ones. Furthermore, thermal comparator techniques can be also employed [106]. Among the possible experimental methods to assess the thermal conductivity of nanofluids, transient hot wire is the most adopted one [44, 51]. Specific heat capacity

of nanosuspensions is typically measured by differential scanning calorimeter [107–109]; whereas viscosity by piston-type [110], capillary [111] or rotational [112] viscometers. Finally, density of nanosuspensions can be evaluated by pycnometers or oscillating U-tube technique [113, 114].

2.2. Experimental evidences

Nanosuspensions were originally investigated as novel heat transfer fluids, because of their effective thermal conductivity (k_{ns}) which is found to be enhanced respect to base fluid one (k_{bf}) [8, 51]. For example, up to 40% thermal conductivity enhancement (k_{ns}/k_{bf}) was reported for a suspension of 0.3% Cu nanoparticles in ethylene glycol [115], whereas 30% enhancement was achieved with 4.3% Al_2O_3 nanoparticles [116]. In average, studies with different nanoparticle/base fluid combinations and volume concentrations between 0.5–4% have generally found 15–40% thermal conductivity increases [3]. While some studies reported thermal conductivity enhancements apparently beyond the classical Maxwell's limit [117, 118], other investigations found good agreement with classical models [76, 119]. Nowadays, an emerging consensus is being reached that these discrepancies arise from the different methods (and surfactants) adopted in nanofluid synthesis, which significantly alter the particle aggregation phenomena and thus compromise the hypothesis of well-dispersed nanoparticle suspensions underlying classical models [8, 63]. However, while the production and physical understanding of well-dispersed colloids have achieved a fair maturity, targeted nanoparticle configurations in base fluids and the involved phenomena therein are still extensively investigated, in order to achieve a good compromise between thermal conductivity and viscosity enhancements [8, 61, 63]. Hundreds of research articles and several reviews have reported thermal conductivity of nanofluids with different geometrical, physical and chemical characteristics [3, 44–46, 50, 51, 53, 59, 62, 120, 121]; here, only a brief summary of the main effects on thermophysical properties of nanosuspensions is presented.

Concerning geometrical characteristics, thermal conductivity of nanosuspensions increases with the volume concentration of nanoparticles, with either linear or nonlinear correlation [51, 122]. The nanoparticle size is also strongly influencing k_{ns}. Most of the studies agrees on larger thermal conductivities of nanosuspensions with decreasing nanoparticle diameter [123, 124], but opposite trends can be also found in the literature [53, 125]. Moreover, also the particle shape is observed to affect k_{ns}, being nanosuspensions with rod-shaped nanoparticles typically characterized by larger thermal conductivity enhancements [126–128]. This may be due to the eased creation of percolation paths and to the higher thermal conductivity in the elongated direction [51, 53]. The particle aggregation is clearly related to k_{ns}; however, while controlled nanoparticle clustering can lead to increased thermal conductivity of nanosuspension [73, 129, 130], severe aggregation may end up with particle sedimentation and thus nanofluid degradation [131, 132]. Regarding chemical features, nanoparticle material

affects k_{ns}: materials with high thermal conductivity (e.g. carbon nanotubes, metals) generally show larger k_{ns}/k_{bf} enhancements [53]. Similar trends should be expected with the thermal conductivity of base fluid [59]. In addition, different base fluids may show different viscosity, therefore affecting the nanoparticle dynamics and thus k_{ns} [133]. Surface functionalization, pH and addition of additives strongly modify k_{ns}/k_{bf}, because they control the solubility and suspension of nanoparticles and thus the resulting clustering events [104, 115, 134–136]. In particular, surfactant concentrations above the Critical Micelle Concentration (CMC) lead to nanofluid degradation and consequent k_{ns}/k_{bf} drop [137]. Physical conditions also influence k_{ns}. In fact, temperature plays a significant role in the Brownian motion and aggregation of suspended nanoparticles [103, 138]. The general trend reported in the literature is a k_{ns}/k_{bf} increase with temperature [53, 139].

Other thermal properties of nanosuspensions are altered respect to the base fluid's ones. On the one hand, the presence of nanoparticles in the proximity of a heated wall contributes to disrupt the boundary layer and then to generally increasing the convective thermal transport [140], especially in developing laminar flows [141]. However, the convective heat transfer coefficient (h_{ns}) of nanosuspensions has shown controversial values in the literature [8]. On the other hand, radiative properties of nanosuspensions are only recently starting to receive attention, particularly for solar applications [142, 143]. Nanoparticle suspensions show also enhanced (25%–250% [8]) Critical Heat Flux (CHC) in pool boiling conditions [144, 145], because of the nanoparticles deposition on the boiling surface which increases the nucleation sites [146]. However, contrasting effects have been reported regarding the possible heat transfer enhancement in the nucleate boiling regime by nanoparticle suspension, namely either positive [147, 148] or negative [146, 149] ones. This discrepancy may be due to different surface wettability and roughness of the nanoparticles considered in the studies [8]. The specific heat capacity of the nanoparticle suspension ($c_{p,ns}$) is typically lower than the pure liquid one, since specific heat of liquids is larger than that of solids [150, 151]. Hence, the reduced heat capacity of nanofluids hampers the possibility to employ them as novel coolants. Moreover, $c_{p,ns}$ is observed to increase with temperature [150] and decreasing particle size [152]. The addition of nanoparticles also affects the thermal expansion of the base fluid [153, 154] and the latent heat of phase change materials [155, 156].

In the overall evaluation of nanofluid performances, non-thermal properties should be also considered. For example, viscosity is essential to determine the adequate pumping power, which contributes to define the efficiency of nanosuspensions in thermal applications. Viscosity significantly increases with nanoparticle concentration [128, 157], and it is also influenced by particle size and shape [128, 158], aggregation [59], pH [159, 160], surfactants [161, 162] and temperature [110, 163]. Moreover, a critical temperature beyond which the viscosity of the nanoparticle suspension dramatically changes has been also observed [110]. Further information regarding the viscosity of nanosuspension can be found in references [96, 164–167]. Finally, the density of nanosuspensions is generally close to that of the base fluid [59], whereas the addition of nanoparticles changes the

surface tension of the base fluid [144, 168].

2.3. Classical and semi-empirical models

The current understanding of the effective thermal conductivity of nanosuspensions comes from continuum-inspired phenomenological formulations, such as Effective Medium Theory (EMT), which usually consider only the shape of the suspended particles and their volume fraction as variables [169]. In this classical formulation, diffusive heat transport is assumed in both liquid and solid phases, while nanoscale phenomena involved in nanosuspensions are typically neglected. As a consequence, classical EMT models often fail to describe thermal conductivity enhancements experimentally observed in nanofluids [43]. Hence, several studies have been devoted to introduce these nanoscale effects in the classical EMT model, in order to provide a better explanation of the thermal transport in nanosuspensions. These mechanisms include liquid nanolayering [43, 170, 171], particle aggregation [43, 73, 74, 171, 172] and the thermal boundary resistance [173]. Moreover, although the fever linked to the micro-convection effect is softened, a number of studies underlining the importance of Brownian motion can be also found [174–179]. Here, we report a selection of EMT models adopted to predict thermal conductivity of nanosuspensions, whereas detailed studies can be found in references [44, 51, 59, 62, 180, 181].

The classical modeling of effective thermal conductivity of nanoparticle suspensions is based on the analysis of Maxwell for solid-liquid mixtures [182]. Despite the model was initially conceived for particles with micrometric size, the Maxwell-Garnett (MG) model has shown good prediction capabilities at low volume concentrations and ambient conditions also with suspension of spherical nanoparticles:

$$k_r = \frac{k_{ns}}{k_{bf}} = \frac{k_p + 2k_{bf} + 2(k_p - k_{bf})\phi}{k_p + 2k_{bf} - (k_p - k_{bf})\phi} \quad , \tag{1}$$

where k_r is the thermal conductivity and ϕ the volume fraction of particles. The limitation on the low ϕ present in the MG model has been addressed by Bruggeman (BG) model, where the interactions among the randomly suspended nanoparticles are also taken into account:

$$\phi \left(\frac{k_p - k_{ns}}{k_p + 2k_{bf}} \right) + (1 - \phi) \left(\frac{k_{bf} - k_{ns}}{k_{bf} + 2k_{ns}} \right) = 0 \quad . \tag{2}$$

Furthermore, the model developed by Hamilton and Crosser (HC) considers the particle shape as an important parameter in the determination of the thermal conductivity of nanosuspension [183], namely:

$$k_r = \frac{k_p + (n-1)k_{bf} - (n-1)(k_{bf} - k_p)\phi}{k_p + (n-1)k_{bf} + (k_{bf} - k_p)\phi} \quad , \tag{3}$$

being $n = 3/\psi$ the shape factor. Note that the sphericity ψ is the ratio between the equivalent sphere surface and the actual particle surface, at fixed volume [128]. Starting

from classical EMT models, several authors have suggested modifications and extensions to include further geometrical, chemical and physical characteristics of nanosuspensions (see a detailed list in reference [46]). For example, Yu and Choi investigated the effect of liquid nanolayer (i.e. liquid molecules in the proximity of nanoparticle surface showing solid-like structures) on the effective thermal conductivity of nanosuspensions [170]; Xuan *et al.* the Brownian motion of nanoparticles and the resulting aggregation phenomena [133]; Murshed *et al.* the particle size, surface chemistry, Brownian motion and nanolayer [184]; Kumar *et al.* the base fluid viscosity and temperature [176]; Hesselman and Johnson the Kapitza resistance at the solid-liquid interface [185]; Wang *et al.* the effect of particle clustering and their distribution [186].

On the other hand, semi-empirical models have been also introduced to fit experimental thermal conductivity of particular nanosuspensions (see a comprehensive overview in reference [51] and [62]). For instance, Corcione proposed an empirical model based on a large amount of experimental data in the literature (and thus with wide regions of validity) [187]; Chon *et al.* an experimental correlation based on Buckingham-Pi theorem for the thermal conductivity of Al_2O_3 nanofluids [188]; Timofeeva *et al.* an experimental relation between thermal conductivity, shape and surface effects of suspended nanoparticles [128]; Khanafer and Vafai a semi-empirical correlation for Al_2O_3 and CuO nanofluids accounting for volume fraction and nanoparticle diameter [46].

The specific heat capacity of nanosuspensions, instead, has been generally predicted by two models. The first one was first introduced by Pak and Cho [189] and then successfully adopted in several studies [103, 190], and it is similar to mixing theories for ideal gas mixtures:

$$c_{p,ns} = (1 - \phi)c_{p,bf} + \phi c_{p,p} \quad , \tag{4}$$

being $c_{p,bf}$ and $c_{p,p}$ the base fluid and particle specific heat capacity, respectively. The second model has found better agreement with experimental results [191–193], and it is derived by classical and statistical mechanics while considering thermal equilibrium between base fluid and particles:

$$c_{p,ns} = \frac{(1 - \phi)(\rho c_p)_{bf} + \phi(\rho c_p)_p}{\rho_{ns}} \quad , \tag{5}$$

where $(\rho c_p)_{bf}$ and $(\rho c_p)_p$ are the volumetric heat capacities of base fluid and nanoparticles [150, 194]. In good agreement with experiments [189, 195], the nanosuspension density is generally estimated as [189, 195]:

$$\rho_{ns} = (1 - \phi)\rho_{bf} + \phi\rho_p \quad , \tag{6}$$

where ρ_{bf} and ρ_p are the densities of base fluid and particles, respectively. However, equations 4 and 5 may sometimes show non-negligible deviations from experimental results [150, 196, 197]; therefore, more accurate semi-empirical models can be also adopted for specific configurations [151]. Note that expressions similar to equations

4 and 5 are also employed for modeling the thermal expansion coefficient of nanosuspensions [198, 199].

Finally, several models of viscosity have been adopted to predict the effective viscosity of nanosuspensions. First, the Einstein model [200] for suspensions of infinitely diluted ($\phi \leq 0.02$) rigid spheres in a viscous fluid is obtained by phenomenological hydrodynamic equations, namely

$$\mu_r = \frac{\mu_{ns}}{\mu_{bf}} = 1 + 2.5\phi \quad , \tag{7}$$

where μ_{bf} and μ_{ns} are the viscosity of base fluid and nanosuspension, respectively. Aiming to extend the validity of Einstein's analysis towards larger particle concentrations, several models have been developed and compared with experiments. For example, Brinkman extended Einstein model to $\phi < 0.04$ [201]:

$$\mu_r = \frac{1}{(1-\phi)^{2.5}} = 1 + 2.5\phi + 4.375\phi^2 + ... \quad ; \tag{8}$$

whereas Lundgren generalized ($\phi < 0.35$) the Brinkman's approach by a Taylor series expansion [202], namely

$$\mu_r = \frac{1}{1 - 2.5\phi} = 1 + 2.5\phi + 6.25\phi^2 + ... \quad . \tag{9}$$

Equation 9 is in good agreement with results from Batchelor studies on Brownian motion of suspensions of rigid spherical particles [203]. On the other hand, Graham modeled the viscosity of nanosuspensions by considering the energy dissipation rate in a fluid cell [204]:

$$\mu_r = 1 + 2.5\phi + 4.5 \left[\frac{1}{(\frac{h}{d_p})(2 + \frac{h}{d_p})(1 + \frac{h}{d_p})^2} \right] \quad , \tag{10}$$

where h is the average interparticle distance and d_p the particle diameter. Theoretical models for the viscosity of nanosuspensions can also include the effect of particle aggregation [205–207]. Moreover, several semi-empirical models have been proposed to fit experimental viscosity of nanoparticle suspensions [46, 110, 140, 197, 205, 208–211]. Further theoretical and semi-empirical models for the viscosity of nanoparticle suspensions can be found in reference [46].

3. Mass transport phenomena in nanoparticle suspensions

Thermal transport phenomena in nanoparticle suspensions are definitely influenced by physical and chemical characteristics of the base fluid as well as by nanoparticle dynamics. On the one hand, the peculiar properties of water molecules at the solid-liquid interface can drastically modify the heat exchange between solid and liquid phase, thus altering the overall properties of the suspension. On the other hand, particle aggregation and clustering are the main responsible of the thermal percolation path creation along

the particle aggregates. In this section, we first review the water molecules dynamics in the proximity of nanoparticle surface. The physics underlying nanolayer formation are explained and the main properties of water at the interface described. Second, we focus on the kinetic of particle aggregation, by reviewing the fundamental theories dealing with particle clustering.

3.1. Water nanolayer

The effect of nonbonded interactions between solid and solvent atoms is strongly intensified at the interface, where liquid molecules, subject to Coulomb and Van der Waals forces, show a reduced mobility and form a structured solid-like layer (i.e. nanolayer) around the particle surface (figure 1). For this reason, the properties of water at solid-liquid nanoscale interface are significantly different from those in the bulk region, and they have been extensively investigated, both experimentally and theoretically [99, 212–214]. Puliti *et al.* [212] studied the nanolayer in gold-water
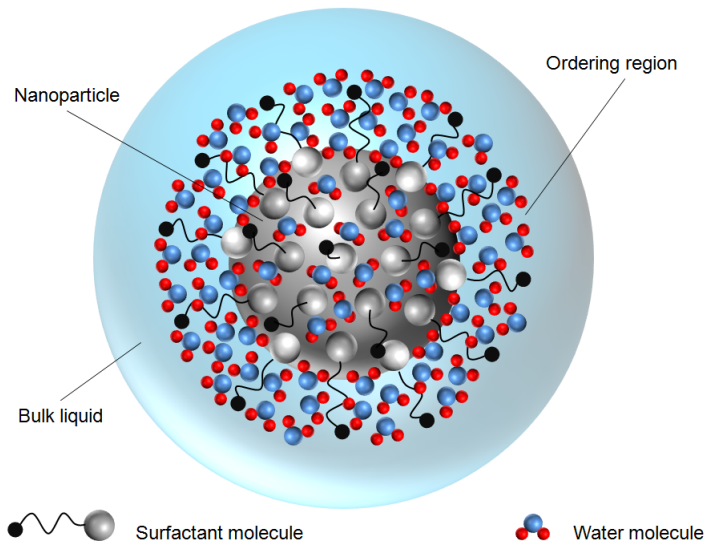
Figure 1. Liquid layering around Al_2O_3 nanoparticle coated by surfactant in aqueous media. The figure takes inspiration from the results of [214–216].

mixtures by Molecular Dynamics (MD) simulations. They observed an increase of water density close to the gold surfaces, up to 0.7 nm away from the solid-liquid interface. They attributed this effect to the more ordered structure of water molecules in the proximity of the metallic surface. Chiavazzo *et al.* [213] and Fasano *et al.* [217] performed MD simulations to evaluate the self-diffusion coefficient (D) of water molecules in different nanoconfined configurations. They systematically calculated the diffusion coefficients within nanopores, around nanoparticles and within nanopores filled by magnetic nanoparticles. In order to provide more general insights, they also evaluated the self-diffusion coefficient within carbon nanotubes (CNTs) and in the proximity of proteins. According to their studies, the nanoconfined water in the nanolayer

region shares some features with supercooled water. Moreover, they found that the self-diffusion coefficient of water in the proximity of solid surfaces scales with a non-dimensional parameter (θ) as (figure 2):

$$D(\theta) = D_b \left[1 + \left(\frac{D_c}{D_b} - 1 \right) \theta \right] \quad , \tag{11}$$

where D_b and D_c are the self-diffusion coefficient of bulk water and completely confined water (i.e. in the nanolayer region) respectively.

Regarding the experimental evidence of nanolayer, Gerardi *et al.* [214] studied the
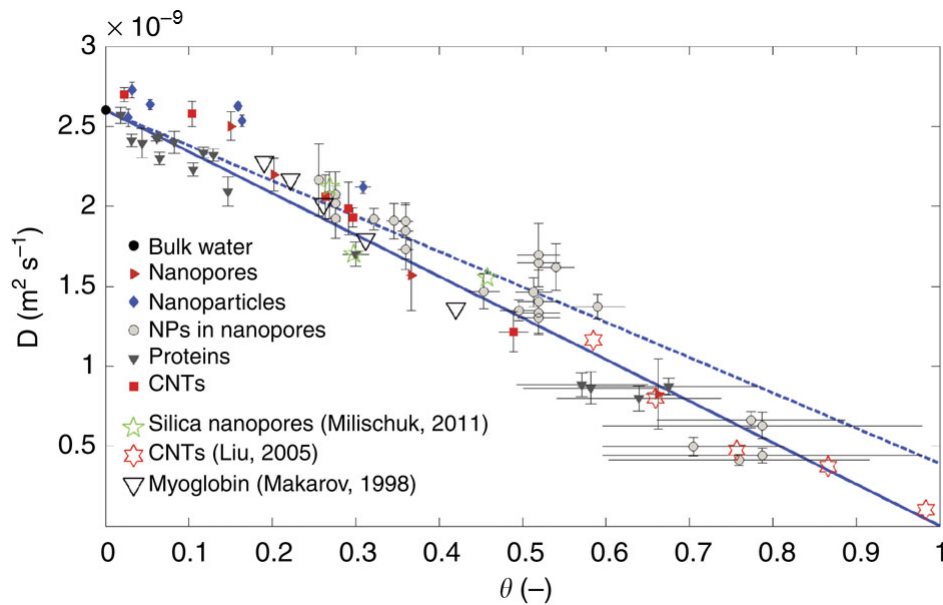
Figure 2. Scaling behavior for the water self-diffusion coefficient (D). The solid and the dashed lines represent equation (11) for $D_c = 0$ and $D_c = 0.39 \times 10^9$ m²s¹, respectively. Figure adapted from reference [213].

liquid layering in alumina-water nanosuspension. In this study, they measured the overall self-diffusion coefficient of water, D, by using nuclear magnetic resonance (NMR). They found that D decreased by increasing the particle volume fraction. The latter evidence was attributed to the increased tortuosity of the water molecules diffusion path, which is due to both the nanoparticle obstacle and to the liquid layering around the particle surface. Gerardi modeled D of water as:

$$D = (1 - P_{bound})D_{free} + P_{bound}D_{bound} \quad . \tag{12}$$

In the previous relation, P_{bound} is defined as the fraction of water molecules in the nanolayer and D_{free} is the self-diffusion coefficient for the free (i.e. not bound to the particles) molecules, which accounts for the effect of tortuosity, namely:

$$D_{free} = \frac{D_b}{1 + \phi/2} \quad . \tag{13}$$

D_{bound}, instead, is the self-diffusion coefficient of non-free (i.e. bound to the particles) water molecules, and it is equal to the self-diffusion coefficient given by Einstein-Stokes relation for the Brownian motion of particles (equation (29)). Based on equation (12) and experimental results, Gerardi and colleagues estimated a nanolayer thickness of about 1.4 nm, which is approximately equal to five layers of water molecules (figure 1). In another work, Turanov and Tolmachev [218] used the NMR approach to measure the self-diffusion coefficient of water in silica nanoparticle suspensions. They estimated a nanolayer thickness of about 1.67 nm, which is almost equal to six molecular layers of water around silica nanoparticles.

Besides density and self-diffusivity, several works focused on the water viscosity at solid-liquid interface [219, 220]. Experimental and theoretical studies have both demonstrated that the viscosity of water in the proximity of hydrophilic surfaces may be orders of magnitude larger than the bulk one [221]. According to the classical Stokes-Einstein relation, self-diffusivity and viscosity of water are inversely proportional; however, it has been demonstrated that supercooled water violates such relation [222–224]. In particular, Stanley and colleagues have found that below a crossover temperature $T \sim 290$ K, the Stokes-Einstein relation $D \sim \mu^{-1}$ is replaced by a "Fractional Stokes-Einstein relation", $D \sim \mu^{-k}$, where k is a characteristic parameter of the medium [225]. Hence, according to the similarities between supercooled and nanoconfined water transport properties, viscosity and self-diffusivity of water in the proximity of a solid surface can present remarkable differences from the bulk region.

3.2. Particle aggregation kinetics

The mass transport phenomena in nanosuspensions mainly involve the nanoparticles dynamics and their aggregation. This mechanism can be described by Smoluchowski equation [226, 227], where the agglomeration frequency (k_{ij}) for a pair of particles i and j is expressed as:

$$k_{ij} = \frac{\beta_{ij}}{W_{ij}} \quad .$$
(14)

β_{ij} is the collision frequency function, which arises from Brownian motion [228, 229], whereas W_{ij} is the stability ratio, namely:

$$W_{ij} = 2 \int_2^\infty \frac{\exp\left(\frac{E_{tot,ij}}{k_B T}\right)}{s^2} ds \quad ,$$
(15)

being $E_{tot,ij}$ the total interaction energy between the particle pair, k_B the Boltzmann constant and s the separation distance between the particles. Thus, only "successful" collisions can lead to coagulation events, while the rate of aggregation strongly depends on E_{tot}.

In colloidal science, the milestone for understanding the interaction energy between suspended particles is the DLVO theory, so called because of the pioneering work by Derjaguin, Landau, Verwey and Overbeek [230–232]. According to such theory, the

interparticle energy depends on the sum of attractive and repulsive interactions, which are both function of particle distance:

$$E_{tot} = E_{vw} + E_{elec} \quad . \tag{16}$$

The London-van der Waals contribution, E_{vw}, between two particles of the same material was derived by Hamaker [233], and it is always attractive thus promoting the aggregation of suspended particles. Instead, the repulsive component of the DLVO theory, E_{elec}, can be explained by recalling the electric double layer formation, i.e. the chemical phenomena occurring on particle surface in a polar host fluid. In such conditions, the nanoparticle develops a surface charge according to the particle material. For example, in case of metal oxides, the charge formation is due to the hydroxylation of their surfaces, which can then react with either H_3O^+ or OH$^-$ in water [234]. The consequent protonation or deprotonation of the surface group results in the positive or negative charge on the particle surface [235]. Instead, in case of functionalized carbon-based particles dispersed in water, a negative surface charge is developed on the particle's surface by the ionization of the surface groups (e.g. -COOH). Because of the surface charge, an electrostatic potential is created in the proximity of nanoparticle, and a concentrated layer of counter ions, known as Stern layer, is formed. Moreover, a Diffuse layer of anions and cations is observable beyond the Stern layer (figure (3)). The charged surface, the Stern layer and the Diffuse layer constitute the three levels of the electric double layer (EDL) typically observed around a solvated nanoparticle [236]. It is worth to notice that the strength of the surface potential can be adjusted by experimentally tuning the pH value of suspension [99, 237, 238]. Based on equation (16), when the electrostatic component is prevailing, particles repel each other, and the potential barrier prevents the particles to agglomerate in the primary minimum. On the other hand, if the van der Waals contribution is dominating, particles can overcome the potential barrier and agglomerate in the primary minimum (figure 4) [234]. Although DLVO theory is considered a stable theory for modeling colloidal interactions, several works have been carried out for including steric [239–242] and hydration [243, 244] contributions in the base theory. In particular, the effect of surfactants can strongly modify the interaction energy between suspended nanoparticles, therefore influencing the aggregation kinetics [245].

The effect of interaction energies between particles can be quantified by zeta-potential (ζ). This potential depends on both particle characteristics and the solution ionic composition (i.e. pH) [246]. The pH value corresponding to $\zeta = 0$ mV is known as the isoelectric point (IEP). When the magnitude of the zeta-potential is smaller than a certain threshold (e.g., $\zeta \approx 10$ mV for Al$_2$O$_3$-water suspensions [246]), the repulsive forces between particles are weak, and particle agglomeration occurs.
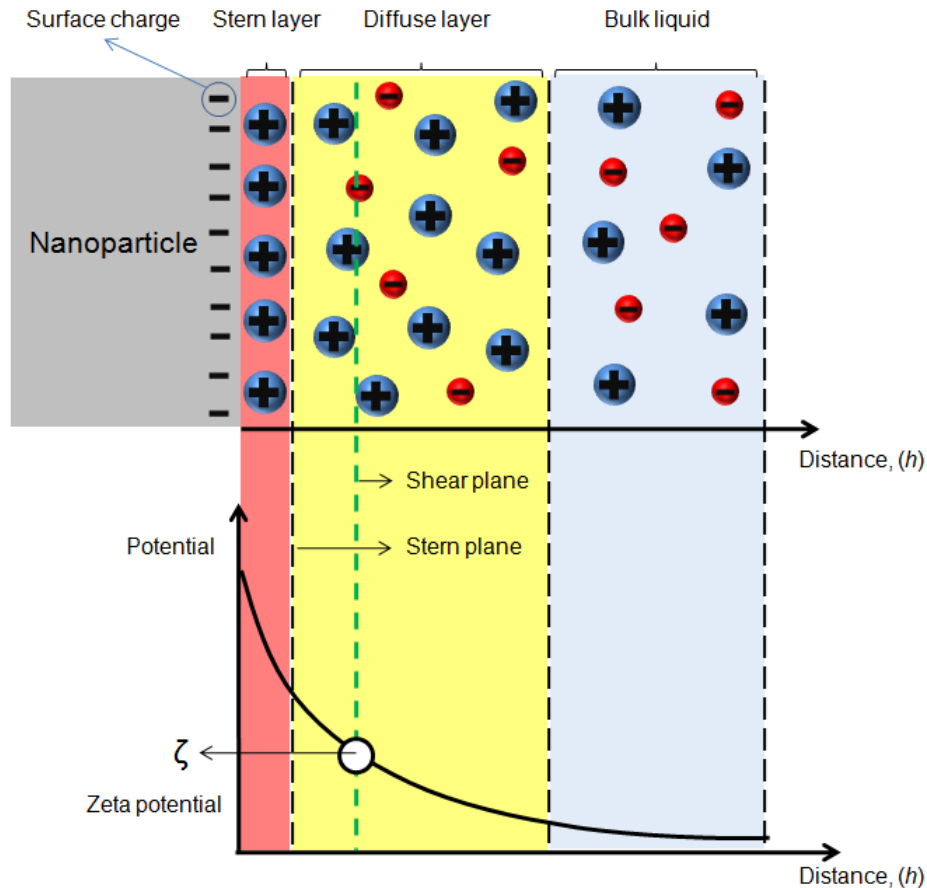
Figure 3. Electric double layer in a polar liquid. Figure reproduced based on reference [234].

4. Thermal transport phenomena in nanoparticle suspensions

In this section, the main thermal transport mechanisms occurring in nanoparticle suspensions are reviewed. A special emphasis is given to the effective conductivity of colloidal suspensions, and to the effect of mass transport phenomena on heat exchange. Hence, nanoscale thermal conduction, micro-convection and percolation effects are studied for a comprehensive understanding of the overall conduction in nanosuspensions. A brief analysis of the radiative heat transfer phenomena concludes the section.

4.1. Conductive heat transfer

Conduction phenomena in nanoparticle suspensions have been extensively investigated in the last decades [3, 5, 7, 43–48]. If thermal conduction within the single phases can be considered as straightforward, it results particularly complex when the overall mixed system is considered. Moreover, the size of the particles, their diffusion and aggregation phenomena make more difficult the understanding of thermal conduction in nanosuspensions. It is evident that a clear scenario of the energy transport mechanisms
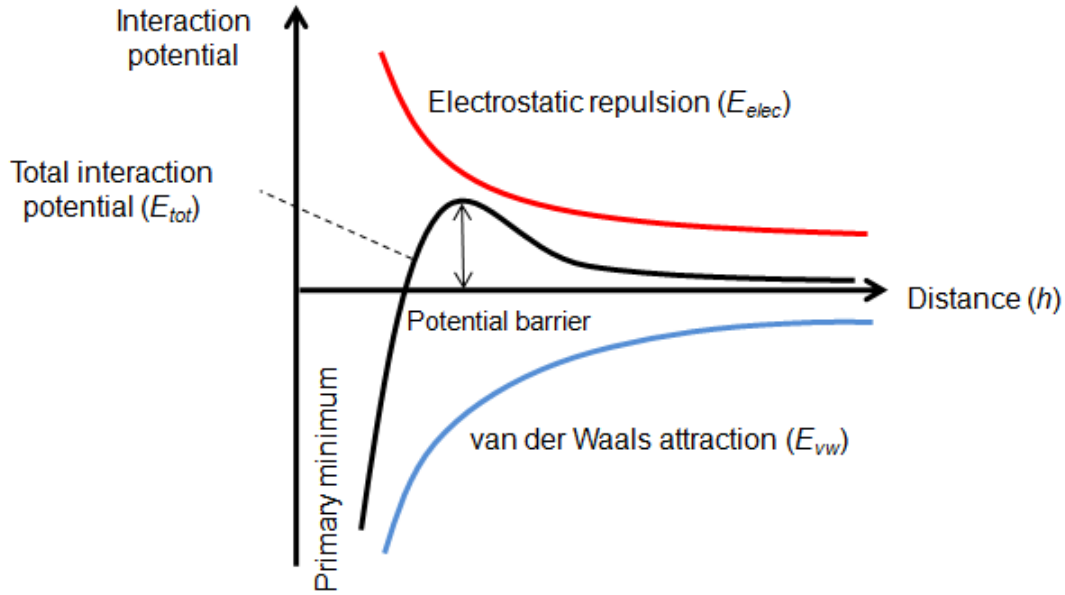
Figure 4. Interaction energy for the stable dispersion of nanoparticles in a liquid medium according to the classical DLVO theory. Figure reproduced based on references [159, 234].

in colloidal systems would allow to accurately define the overall thermal conductivity, hence to study the temperature trends in heat exchange applications.

4.1.1. Nanoscale heat transfer
  Thermal conduction within the nanoparticles is a typical phenomena occurring in size-affected domains, where the classical governing laws, such as Fourier's law, break down because of the small size. Nanoscale heat transfer in colloidal suspensions is usually better described by discrete particle-based descriptions rather than continuum approaches. In order to identify the nanoscale heat transfer regime, a comparison between the typical size of system and the characteristic length scales of energy carriers is required. Recalling the wave-particle duality of energy carriers, the characteristic length scales can be associated either to the mean free path, i.e. the average distance between successive collisions of the energy carriers, or to the average wavelength of phonons. For the former case, the mean free path Λ can be estimated as:

$$\Lambda = \frac{kmv_F}{\pi^2 n k_B^2 T} \quad \text{(electrons in metals particles)} \quad , \tag{17}$$

$$\Lambda = \frac{3k}{\int_0^{\omega_{max}} C_\omega v_\omega d\omega} \quad \text{(phonons)} \quad , \tag{18}$$

being C the volumetric specific heat, v the velocity of the carriers, m the energy carriers mass and k the thermal conductivity. For the latter case, instead, the average wave

length is given by:

$$\lambda = \frac{2hv}{k_B^2 T} \quad , \tag{19}$$

where h is the Planck's constant. A third characteristic length scale considers the coherence length in optics, which takes into account the spread in energy of the wave packets:

$$l_c = \frac{c}{\Delta v} \quad , \tag{20}$$

where c is the speed of light and Δv is the bandwidth of radiation. Thus, the comparison between the typical size of colloids and the above mentioned lengths allows to tune the correct techniques for describing thermal conduction within nanoparticles.

4.1.2. Effect of thermal boundary resistance

A complete analysis of nanoscale heat transfer in nanosuspensions should also include thermal mechanisms at the solid-liquid interface and across the solvent nanolayer. For example, the interfacial thermal resistance, also known as Kapitza resistance (R_k), plays a fundamental role in the study of nanoscale heat transport phenomena at interfaces and within particle suspensions. From a theoretical point of view, two model are adopted to describing interfacial thermal resistance: the acoustic mismatch model (AMM), which accounts for long-wavelength phonons; the diffuse mismatch model (DMM), which assumes a complete diffuse scattering at the interface. However, both AMM and DMM model do not include details of the interfacial nanostructure: in both models, thermal boundary resistance is only determined by the materials of phases in contact, without considering the nature of the joint. For this reason, experimental, computational and semi-empirical nanoscale techniques are preferred for studying thermal transport at solid-liquid interfaces.

In general, Kapitza resistance is due to local phonon scattering at the interface of dissimilar materials, e.g. at the particle-fluid interface in nanosuspensions [68, 173, 247–249]. It is worth to underline that Kapitza resistance exists even at atomically perfect interfaces and, therefore, it is different from contact resistance, which is due to poor mechanical connections between two materials [173, 250]. Generally, Kapitza resistance is expressed as:

$$R_k = \frac{1}{G_k} = \frac{\Delta T}{q} \quad , \tag{21}$$

where G_k is the thermal boundary conductance (transmittance), ΔT is the temperature difference between at the interface and q is the heat flux per unit area. Such thermal resistance can be also expressed in terms of Kapitza length (or radius) (l_k), i.e. the equivalent thickness of a bulk material having the same overall thermal resistance of the interface [251, 252]:

$$l_k = R_k k_{bf} = \frac{k_{bf}}{G_k} \quad , \tag{22}$$

being k_{bf} the thermal conductivity of the base fluid or matrix.

For low concentration of well-dispersed spherical nanoparticles, Putnam *et al.* introduced the effect of interfacial thermal resistance in the expression of nanosuspension thermal conductivity [253]:

$$k_r = 1 + 3\phi\frac{\Gamma - 1}{\Gamma + 2} = 1 + 3\phi\frac{\dfrac{r_p}{l_k} - 1}{\dfrac{r_p}{l_k} + 2} \quad , \tag{23}$$

where $\Gamma = G_k r_p/k_{bf}$. Therefore, it is possible to define a critical particle radius equal to the Kapitza length at which there is no heat conduction enhancement. Instead, for particles with radii higher than the Kapitza length, the thermal conductivity of the suspension increases.

Other studies demonstrated that the hydrophobicity or hydrophilicity of the solid surface has a substantial impact on the interfacial thermal resistance [251]. Ge *et al.* experimentally measured the thermal boundary conductance (G_k) for either hydrophilic or hydrophobic Al-water and Au-water interfaces [251]. Specifically, they evaluated the thermal transmittance of the functionalized Al and Au interfaces by considering four heat transport mechanisms:

 (i) heat transport from metal surfaces to functional groups;

 (ii) heat transport across the functional groups;

(iii) heat transport from terminal groups to surrounding confined water;

(iv) heat transport from confined water gap to bulk water.

Based on their measurements, thermal boundary conductance for hydrophobic surfaces was 60 ± 5 MWm^{-2}K^{-1} (Al) and 50 ± 5 MWm^{-2}K^{-1} (Au); while for hydrophilic surfaces G_k=180 ± 30 MWm^{-2}K^{-1} (Al) and G_k=100 ± 20 MWm^{-2}K^{-1} (Au), respectively. From these measures, Ge and co-workers observed that hydrophilic surfaces were characterized by a larger thermal boundary conductance. Thus, such surfaces are preferable for efficient heat conduction in nanosuspension. The large difference between G_k of hydrophobic and hydrophilic interfaces was attributed to the critical role of water layering across the solid-liquid interfaces with different surface properties.

4.1.3. Effect of nanolayer

A number of theoretical and experimental studies have highlighted the effect of solvent nanolayer on the thermal conductive mechanisms within nanosuspensions.

Jiang *et al.* [254] derived a mathematical expression for thermal conductivity of alumina-ethylene glycol nanosuspension. They found that the thermal conductivity of base fluid in the nanolayer region (k_{layer}) was higher than the bulk one, and proved that the effect of liquid layering around nanometer-sized particles was more pronounced for smaller particles.

Yu and Choi [170] also studied the effect of nanolayer on the thermal conductivity enhancement in nanosuspensions. They modeled nanoparticle suspension as a three

phase system, and supposed that the nanolayer could provide a percolation between solid nanoparticles and bulk liquid, thus enhancing the overall thermal conductivity. Yu and Choi also found that the liquid layer (thickness δ) around the particle surface (radius $r_p = d_p/2$) has higher thermal conductivity than the bulk liquid. The nanolayer is added to the particle to form an equivalent particle, with radius $r + \delta$, leading to an increased volume fraction:

$$\phi_e = \frac{4}{3}\pi(r+\delta)^3 N_P = \phi(1+\vartheta)^3 \quad , \tag{24}$$

where N_P is the amount of particles and $\vartheta = \delta/r_p$. The thermal conductivity of equivalent particles, k_{pe}, is then calculated from the effective medium theory as:

$$k_{pe} = \frac{[2(1-\gamma) + (1+\vartheta)^3(1+2\gamma)]\gamma}{-(1-\gamma) + (1+\vartheta)^3(1+2\gamma)} k_p \quad , \tag{25}$$

being $\gamma = k_{layer}/k_p$. Thus, the MG model in the equation (1) was consequently modified as:

$$k_r = \frac{k_{pe} + 2k_{bf} + 2(k_{pe} - k_{bf})(1+\vartheta)^3\phi}{k_{pe} + 2k_{bf} - (k_{pe} - k_{bf})(1+\vartheta)^3\phi} \quad . \tag{26}$$

According to Yu and Choi, the nanolayer behaves as a thermal bridge between nanoparticles, and it is more effective when the nanoparticle diameter is less than 10 nm. Equation (26) is only valid for spherical particles. Hence, to incorporate the effect of non-spherical nanoparticles, Yu and Choi proposed a new expression based on the HC model, which can be found in reference [255].

Xue and Xu [256] modified the BG model in equation (2) by considering the effect of interfacial shells on the thermal conductivity of nanosuspensions. They proposed the following relation for the thermal conductivity of an equivalent particle (k_{pe}):

$$k_{pe} = \frac{2k_{layer} + k_p + 2\alpha(k_p - k_{layer})}{2k_{layer} + k_p - \alpha(k_p - k_{layer})} \quad , \tag{27}$$

where $\alpha = k_p/k_{bf}$. Thus, BG model was modified as:

$$\left(1 - \frac{\phi}{\alpha}\right)\frac{k_{ns} - k_{bf}}{2k_{ns} + k_{bf}} +$$
$$+ \frac{\phi}{\alpha}\frac{(k_{ns} - k_{layer})(2k_{layer} + k_p) - \alpha(k_p - k_{layer})(2k_{layer} + k_{ns})}{(2k_{ns} + k_{layer})(2k_{layer} + k_p) + 2\alpha(k_p - k_{layer})(k_{layer} - k_{ns})} = 0. \tag{28}$$

Using this model, Xue and Xu could analyze the particle size dependence of thermal conductivity for an Al_2O_3-water nanosuspension. They set $\delta = 3nm$ and estimated $k_{layer} = 5$ W/mK, which is lower than Al_2O_3 thermal conductivity (46 W/mK) but higher than that of bulk water (0.604 W/mK). In this analysis, they observed that k_{ns} significantly increases by reducing the particle size.

In order to give further insights into the effect of nanolayer formation in suspended nanoparticles, some researchers performed molecular dynamics analysis. For example,

Li *et al.* [257] investigated the effect of nanolayer on the thermal conductivity of copper-liquid argon nanofluid through molecular dynamics simulations. They observed a thin (about 0.5 nm thickness) ordered layer at the interface and demonstrated the nanolayer contribution to enhancing the overall thermal conductivity of the suspension.

4.1.4. Effect of Brownian motion

Brownian motion of nanoparticles is one of the heat conduction mechanisms proposed for understanding the peculiar thermophysical properties of nanocolloids. A number of models have been developed on the basis of Brownian motion of nanoparticles, which is also known as micro-convection [175, 258, 259].

The particle diffusion within the base fluid continuously favors the heat absorption and release, thus promoting the convective heat transfer and the enhancement of energy transport. Indeed, the phenomenon is strongly enhanced with high temperatures and small particle sizes, as suggested by Einstein-Stokes equation for the diffusion coefficient of the particle [260]:

$$D_p = \frac{k_B T}{3\pi\mu_{nf}d_p} \quad, \tag{29}$$

where, d_p is the nanoparticle hydrodynamic diameter. However, Keblinski *et al.* [43, 63] analyzed the Brownian motion effect on thermal conduction by comparing the time scale of heat diffusion

$$\tau_H = \frac{\rho c_{p,bf}d_p^2}{6k_{bf}} \quad, \tag{30}$$

with the time scale of particle motion in the fluid

$$\tau_D = \frac{3\pi\mu_{bf}d_p^3}{6k_B T} \quad. \tag{31}$$

From equations (30) and (31), they realized that, in case of water at room temperature and particles down to atomic size (e.g. 0.5 nm), Brownian diffusion is much slower than thermal diffusion, namely: $\tau_D/\tau_H \approx 25$. As a result, the heat transferred through base liquid by thermal diffusion is much faster than the heat transfer by nanoparticles diffusion. Other works confirmed the minor role of Brownian motion for explaining the enhanced thermal conductivity in nanosuspensions [178, 261]. For example, Evans *et al.* [178] demonstrated, by means of molecular dynamics simulations, the negligible contribution of hydrodynamic effects on the thermal conduction in nanofluids.

Currently, scientists are paying less attention to micro-convection. On the other side, many works suggest the important effect of Brownian motion on the aggregation of nanoparticles: at constant volume fraction, the probability of particle clustering increases by reducing the particle size. The aggregation in turn causes the decrease of Brownian motion, due to the formation of heavier clusters [232, 262].

4.1.5. Effect of particle aggregation

Aggregation of nanoparticles is a time-dependent phenomenon that strongly affects

the overall thermophysical properties of nanosuspensions [67, 207, 246, 263, 264]. An example of particle aggregation is presented in figure 5.

The effect of aggregation on the effective thermal conductivity of nanoparticle
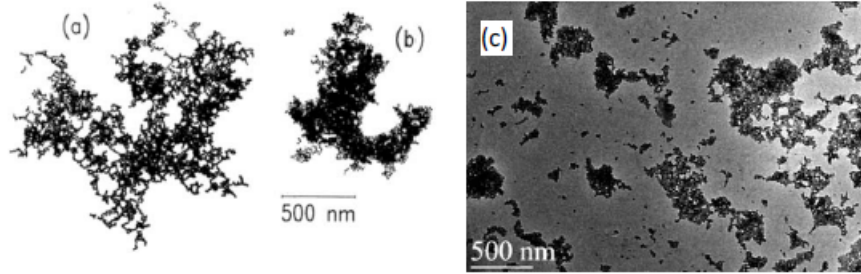
Figure 5. (a) and (b) TEM images of Au clusters [265, 266]. (c) Aggregated ST-40 silica colloid at pH =7.5 after 3 h 15 min since the initial pH adjustment. Figure adapted from reference [265].

suspensions is treated in several experimental and theoretical works [73, 75, 265, 267, 268]. Aggregates provide highly conductive percolation paths enhancing the overall thermal conduction of colloidal suspensions as shown in figure 6.
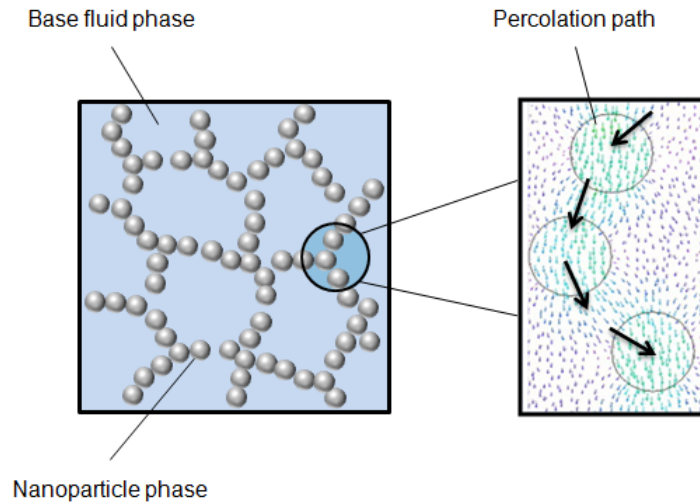
Figure 6. Schematics of the heat conduction percolation path throughout the particle suspension. Figure reproduced has been adapted from references [269, 270].

Starting from the BG formulation and taking into account the theory of completely misoriented ellipsoidal particles [271], Prasher *et al.* evaluated the thermal conductivity of particle aggregates (k_a) as [73]:

$$\phi_{int}\left(\frac{k_p - k_a}{k_{bf} + 2k_a}\right) + (1 - \phi_{int})\left(\frac{k_{bf} - k_a}{k_{bf} + 2k_a}\right) = 0 \quad , \tag{32}$$

where ϕ_{int} is the volume fraction of particles in the aggregates. After calculating k_a from equation (32), they determined the overall thermal conductivity by MG model [73]:

$$k_r = \frac{k_a + 2k_{bf} + 2(k_a - k_{bf})\phi_a}{k_a + 2k_{bf} - (k_a - k_{bf})\phi_a} \quad , \tag{33}$$

where $\phi_a = \phi_p/\phi_{int}$ is the volume fraction of the aggregates and ϕ_p is the volume fraction of nanoparticles. For a fully-aggregate system ($\phi_a = 1$) the volume concentration of nanoparticles is equal to the volume fraction of particles in aggregates ($\phi_{int} = \phi_p$). For a well-dispersed system ($\phi_{int} = 1$) there is only one particle in each aggregate, thus the volume concentration of nanoparticles is equal to the volume fraction of aggregates ($\phi_a = \phi_p$). It has been observed that the maximum thermal conduction occurs between these two limits [73].

Philip *et al.* [267] experimentally studied the thermal conductivity enhancements in aqueous suspensions of magnetite nanoparticles subject to a magnetic field. By increasing the magnetic field, these nanoparticles could align in the direction of the field and form a chain-like structure. In this way, they could accurately evaluate the relation between overall thermal conductivity, nanoparticle aggregation and chain-length. They attributed the improvement of thermal conduction to the formation of chain-like structures promoting thermal percolation paths, as formerly proposed by Prasher *et al.* [73].

Further confirmations of such influence derive from the study by Eapen *et al.* [272], where the Hashin and Shtrikman mean-field bounds model was tested and validated for a large variety of nanosuspensions. Specifically, their results showed good agreement with the model by considering linear-chain like arrangement of nanoparticles rather than well dispersed conditions. Dhar *et al.* [273] also proposed a theoretical model to predict the role of percolation paths for the thermal conductivity enhancement in graphene based nanosuspensions.

Although several works investigated percolation phenomena in nanosuspensions, their effect on the effective thermal conductivity of nanosuspensions has not been fully understood, due to the numerous physical and chemical parameters involved.

4.2. Radiative heat transfer

Among the various thermophysical benefits, the addition of nanoparticles in liquid also offers the potential of improving the radiative absorbing properties of the base fluid [142, 274, 275]. Hence, the use of nanoparticle suspensions for harvesting thermal energy is receiving remarkable attention in the energy field [30, 276–278]. One of the main benefits offered by such suspensions is that nanoparticles are smaller than the mean free path of the incident radiation, thus the scattering is negligible and the absorption spectrum is typically broadened [279], which leads to enhanced absorption efficiency.

The formal light scattering theory is characterized by two theoretical frameworks: the Rayleigh and the Mie scattering theories [279]. Hereby, we present the former one, whereas the latter theory is extensively presented elsewhere [142]. Planck's law describes

the electromagnetic radiation spectrum emitted by a black body (e.g., sun) in thermal equilibrium as a function of wavelength and temperature:

$$I_{b\lambda}(\lambda, T_{sun}) = \frac{2hc^2}{\lambda^5[\exp(\frac{hc_0}{\lambda k_B T_{sun}}) - 1]} \quad , \tag{34}$$

being T_{sun} the surface temperature of the sun, h the Plank's constant, c_0 the light speed in vacuum and λ the radiation wavelength. Within any medium, an attenuation of the total radiation intensity is measured by the Beer-Lambert law:

$$I(\lambda) = I_0(\lambda) \exp^{-L\mu_{(tot,\lambda)}} \quad , \tag{35}$$

where L is the fluid depth and $\mu_{tot} = \mu_{particle} + \mu_{basefluid}$ is the extinction coefficient of the suspension. Specifically, the particle extinction coefficient ($\mu_{particle}$) includes both scattering and absorption contributions, namely:

$$\mu_{particle} = \frac{3}{2} \frac{f_v(Q_{(abs,\lambda)} + Q_{(scat,\lambda)})}{D} \quad . \tag{36}$$

where f_v is the particle volume fraction, $Q_{(sca,\lambda)}$ and $Q_{(abs,\lambda)}$ are the scattering and absorption efficiency, respectively. Both $Q_{(sca,\lambda)}$ and $Q_{(abs,\lambda)}$ strongly depend on the particle size parameter $\alpha = \frac{\pi D}{\lambda}$. In particular, $Q_{(sca,\lambda)}$ is proportional to the fourth power of α. When the particle diameters are much smaller than the wavelength of the incident light and hence in case of nanoparticle, α and consequentially $Q_{(sca,\lambda)}$ are $<< 1$. Therefore, the suspended nanoparticles can be considered as transparent to the elastic collision, and the role of solar absorption is globally enhanced by the suspension.

The large variety of combinations in synthesizing nanosuspensions implies strong sensitivity of the effective optical properties on the physical and chemical characteristics of the suspension; therefore, several studies investigated the optimal nanofluid configuration for solar applications [280, 281].

5. Computational modeling approaches

Computational modeling techniques represent effective tools to observe, describe and understand various thermal physical mechanisms occurring in nanoparticle suspensions. In this section, we review the modeling techniques used for simulating nanoscale and macroscale heat transfer, with particular focus on the simulation of particle aggregation dynamics.

5.1. Nanoscale simulations

Several simulation tools are employed for dealing with nanoscale heat transfer, in particular for studying phonon properties such as density of state, dispersion relation, relaxation time and transmission across interfaces [282–284]. First principle calculations, classical molecular dynamics, atomistic Green's function and Monte Carlo simulations

are some examples of such nanoscale techniques. In the context of particle suspensions, studies on nanoscale heat transport are generally focused on thermal phenomena occurring at solid-liquid interfaces, e.g. thermal boundary resistance at solid-solid and solid-liquid interfaces [72, 285, 286].

Non-equilibrium molecular dynamics (NEMD) and equilibrium molecular dynamics (EMD) simulations are used to calculate thermal transport properties at particle-solvent interface [286, 287], as well as to show the role of particle aggregation in the overall thermal conduction [288, 289]. For example, Zhou *et al.* [286] simulate the heat transfer process from a gold nanoparticle, heated by continuous laser pumping, to a pool of water. Specifically, they showed how particle wettability can strongly influence Kapitza resistance: surface hydrophilicity enhances interfacial interactions, thus increasing the thermal conductance at particle-liquid interface. Such a finding is also confirmed by the MD simulations of Shenogina *et al.* [290]. Desai and coworkers [291] studied by NEMD and EMD the thermal transport phenomena in silicon cluster made of 15 nm diameter nanoparticles, focusing in particular on the effect of ballistic regime within the nanosized neck region.

Lattice dynamics can be also carried out to study nanoscale heat transfer. When combined with first-principle calculations, it has been able to predict phonon properties and thermal conductivity of nanosuspensions with unprecedented accuracy and without any empirical input. [292–294]. However, systems with interfaces and defects cannot be easily simulated by first principle simulations. Thus, an alternative approach to study thermal transport at the nanoscale interface is represented by the Atomistic Greens function method, first developed by Mingo and Yang [295] for modeling electron transport. In such method, the heat current is expressed in term of Green's function, and the phonon transmission is calculated as a function of phonon frequency [296–298].

Although the above methods can model the nanoscale heat transfer phenomena in nanosuspensions, they are intrinsically affected by the small simulation domain. Moreover, the multiscale nature of nanosuspensions requires the integration of several simulation techniques to fully modeling the effect of nanoscale phenomena on overall properties. In other words, nanosuspensions involve length scales much larger than molecular dimensions (i.e. nanoparticles and aggregates, typically in the range 10^8m 10^6m), but small enough to be affected by thermal fluctuations and colloidal forces (i.e. van der Waals dispersion and long-range electrostatic forces). Hence, nanoscale techniques are not enough to fully describe the properties of nanosuspensions, and multiscale simulation tools are needed to bridge the length-scale and time-scale gaps between atomistic simulations and real materials and devices.

5.2. Mesoscale simulations

Modeling the nanoparticle dynamics plays a fundamental role in studying thermal phenomena in colloidal dispersion. We have already stressed that the creation of percolation networks along nanoparticle clusters represents a key mechanism for thermal

conductivity enhancement in nanosuspensions. However, the cluster structures are strongly influenced by several chemical and physical factors, and the hypothesis of randomly orientated particles may easily break down. Consequently, understanding the dynamics of percolation path creation is critical to precisely control and describe the effective thermophysical properties.

A large number of simulation techniques are available to study the dynamics of suspended nanoparticles and their aggregation [299]. A first class of tools includes lattice-based models, where the solvent is treated as lattice (Lattice-Boltzmann techniques [300–303]) or continuum (Navier-Stokes based techniques [304–306]) and the particles are described by immersed boundary method in Brownian motion. The second class, instead, is represented by particle-based methods, where particles are treated explicitly and the solvent is described either as a separate set of particles (explicit) or incorporated in the colloid-colloid interaction (implicit). On one hand, multi-particle collision dynamics (MPCD) [307, 308], originally known as stochastic rotation dynamics (SRD) [309, 310], and dissipative particle dynamics (DPD) [311–313] are some examples of particle based techniques with explicit description of the solvent. In particular, dissipative particle dynamics was developed to overtake the computational limit of MD. The DPD method includes both hydrodynamic and Brownian fluctuations effects on nanoparticles, while the fluid is represented by groups of dissipative particles interacting each other by exchanging momentum. On the other hand, in Fast Lubrication Dynamics (FLD) [314] or Stokesian dynamics (SD) [315] methods, the effect of hydrodynamics is implicitly included in the Brownian motion of the particles. An example of implicit solvent simulations is provided by Liu *et al.* [316, 317], where particle agglomeration is studied by Monte Carlo simulations to include Smoluchowski equation and Brownian motion. Moreover, they investigated the role of the hydration repulsion within the extended version of the classical DLVO theory. Instead, a recent study combining deterministic and stochastic modeling of nanoparticle agglomeration is presented by Mortuza *et al.* [318]. Here, we remark the importance of correctly modeling the interaction potential between nanoparticles because, as pointed out in paragraph 3.2, non-DLVO interactions (i.e., hydration and steric forces) should be also taken into for a realistic modeling of particle kinetic and aggregation.

These simulation techniques provide effective means for predicting suspended particle kinetics and eventually aggregates morphology. Such information is fundamental to evaluate the contribution of thermal percolation paths on the overall thermal conductivity of nanosuspensions [172, 319–321]. For example, by Monte Carlo simulations of aggregate fractal structures, Evans *et al.* [172] provided a first validation of the cluster homogenization theory expressed in equation 33. Specifically, the aggregation phenomena was modeled by a diffusion-limited clustercluster aggregation (DLCCA) algorithm, and the global analysis included the effect of interfacial thermal resistance and cluster aspect ratio. Gharagozloo and colleagues [320, 321] also performed Monte Carlo simulations to model the dynamics of suspended nanoparticles and to calculate the average number of particles in the aggregates, their radius of gyration and

hydraulic diameter. These parameters were then coupled to effective medium theory for the evaluation of the overall thermal conductivity. More precisely, the thermal conductivity of aggregates was calculated by differentiating the percolation contributing backbone and the non-percolation contributing dead-ends: the former is calculated by composite theory for completely misoriented ellipsoidal particles [271]; the latter by the Bruggeman model. The authors demonstrated a good agreement between modeling results and experimental measures.

An interesting study on modeling the thermal conduction along nanostructured aggregates is presented by Sastry *et al.* [322]. This work is based on the formation (percolation) of three-dimensional CNT chains and the calculation of the corresponding thermal resistance network. Results highlighted that the enhancement in thermal conductivity critically depends on the CNT geometry (length), volume fraction and CNT-liquid suspension properties. Other investigations on the effect of percolation in CNT based nanosuspension were carried out by Lamas *et al.* [323].

6. Conclusions and perspectives

This review is focused on the heat and mass transport phenomena occurring in nanoparticle suspensions.

Suspending nanoparticles in traditional heat transfer fluids can be an effective way to enhance their thermophysical properties. Several studies investigated transport phenomena in nanoparticle suspensions, particularly focusing on thermal conductivity and viscosity. However, clear guidelines for a rational design of nanosuspensions are still missing, mainly because of the lack of understanding and control of aggregate morphology and dynamics on suspension stability and thermal properties. Hence there is a need for bottom-up predictive models including all relevant molecular effects.

One of the main modeling issues is the pronounced sensitivity of the suspension properties and particle aggregation on the characteristics of their constituents, namely particle material, shape, size and volume fraction, as well as base fluid, pH and surfactant concentration. In this sense, the first step to predict the effective mean-field properties of nanosuspensions is provided by the effective interaction potential between the nanoparticles. Typically the standard DLVO theory only provides a qualitative understanding of such interaction potential. However, additional non-DLVO forces should be also considered for a more quantitative modeling of colloidal stability and nanoparticle aggregation. For example, the hydration forces arising in the nanoscale gaps between approaching nanoparticles should be properly modeled. Moreover, when surfactants are added to stabilize and disperse nanoparticles, steric repulsion forces should be also taken into account. Both hydration and steric forces are strongly dependent on the atomistic details of the nanoparticle surface. In the field of computational modelling, one effective tool for evaluating the total interaction potential, including the non-DLVO forces, is represented by the Potential of Mean Forces (PMF) obtained by atomistic calculations [85, 242, 245]. Such PMF can be used to

upscale molecular details in coarse-grained simulations at time and length scales much larger than those of all-atom description, e.g. by accurately driving the dynamics of aggregation in implicit solvent modeling (see equation 15).

The development of multiscale models and better understanding of the effects of particle aggregation are essential and still missing to predict the transport properties of nanosuspension. This would pave the way to a more rational design in a broad range of applications, from biomedicine to engineering.

Acknowledgments

References

[1] Wagner F E, Haslbeck S, Stievano L, Calogero S, Pankhurst Q and Martinek K P 2000 *Nature* **407** 691–692

[2] Heiligtag F J and Niederberger M 2013 *Materials Today* **16** 262–271

[3] Yu W, France D M, Routbort J L and Choi S U 2008 *Heat Transfer Engineering* **29** 432–460

[4] Trisaksri V and Wongwises S 2007 *Renewable and Sustainable Energy Reviews* **11** 512 – 523

[5] Choi S U and Eastman J 1995 Enhancing thermal conductivity of fluids with nanoparticles Tech. rep. Argonne National Lab., IL (United States)

[6] Yu W, France D M, Routbort J L and Choi S U 2008 *Heat Transfer Engineering* **29** 432–460

[7] Saidur R, Leong K and Mohammad H 2011 *Renewable and Sustainable Energy Reviews* **15** 1646–1668

[8] Taylor R, Coulombe S, Otanicar T, Phelan P, Gunawan A, Lv W, Rosengarten G, Prasher R and Tyagi H 2013 *Journal of Applied Physics* **113** 011301

[9] Borbáth T, Bica D, Potencz I, Vékás L, Borbáth I and Boros T 2010 Magnetic nanofluids and magnetic composite fluids in rotating seal systems *IOP Conference Series: Earth and Environmental Science* vol 12 (IOP Publishing) p 012105

[10] Choi C J, Jang S P and Choi S U 2011 *Journal of Colloid and Interface Science* **363** 59 – 63

[11] López T D F, González A F, Del Reguero Á, Matos M, Díaz-García M E and Badía-Laíño R 2016 *Science and Technology of Advanced Materials*

[12] Suleimanov B, Ismailov F and Veliyev E 2011 *Journal of Petroleum Science and Engineering* **78** 431–437

[13] Du Y, Lv Y, Li C, Chen M, Zhong Y, Zhou J, Li X and Zhou Y 2012 *Dielectrics and Electrical Insulation, IEEE Transactions on* **19** 770–776

[14] Maeda K, Teramura K, Lu D, Takata T, Saito N, Inoue Y and Domen K 2006 *Nature* **440** 295–295

[15] Kudo A and Miseki Y 2009 *Chemical Society Reviews* **38** 253–278

[16] Roy S C, Varghese O K, Paulose M and Grimes C A 2010 *Acs Nano* **4** 1259–1278

[17] Li Y and Somorjai G A 2010 *Nano letters* **10** 2289–2295

[18] Venkatesan S and Kadiresh P 2014 *International Journal of Ambient Energy* 1–4

[19] Liu B T and Yeh W D 2010 *Colloids and Surfaces A: Physicochemical and Engineering Aspects* **356** 145–149

[20] Ogihara H, Okagaki J and Saji T 2011 *Langmuir* **27** 9069–9072

[21] Chantrell R, Popplewell J and Charles S 1978 *Magnetics, IEEE Transactions on* **14** 975–977
[22] Chantrell R and Wohlfarth E 1983 *Journal of magnetism and magnetic materials* **40** 1–11
[23] Chantrell R, Walmsley N, Gore J and Maylin M 2000 *Physical Review B* **63** 024410
[24] Torres-Díaz I and Rinaldi C 2014 *Soft matter* **10** 8584–8602
[25] Neumann O, Urban A S, Day J, Lal S, Nordlander P and Halas N J 2012 *Acs Nano* **7** 42–49
[26] Neumann O, Feronti C, Neumann A D, Dong A, Schell K, Lu B, Kim E, Quinn M, Thompson S, Grady N *et al.* 2013 *Proceedings of the National Academy of Sciences* **110** 11677–11681
[27] Ni G, Miljkovic N, Ghasemi H, Huang X, Boriskina S V, Lin C T, Wang J, Xu Y, Rahman M M, Zhang T *et al.* 2015 *Nano Energy* **17** 290–301
[28] Lenert A and Wang E N 2012 *Solar Energy* **86** 253–265
[29] Colangelo G, Favale E, Miglietta P, de Risi A, Milanese M and Laforgia D 2015 *Applied Energy* **154** 874–881
[30] Moradi A, Sani E, Simonetti M, Francini F, Chiavazzo E and Asinari P 2015 *Journal of nanoscience and nanotechnology* **15** 3488–3495
[31] Leong K, Ong H C, Amer N, Norazrina M, Risby M and Ahmad K K 2016 *Renewable and Sustainable Energy Reviews* **53** 1092–1105
[32] Novak E V, Pyanzina E S and Kantorovich S S 2015 *Journal of Physics: Condensed Matter* **27** 234102
[33] Liu J, Yan J F and Deng Z S 2007 *ASME 2007 International Mechanical Engineering Congress and Exposition* 87–94
[34] Zhang L, Ding Y, Povey M and York D 2008 *Progress in Natural Science* **18** 939–944
[35] Barnard A S 2015 *Journal of Physics: Condensed Matter* **28** 023002
[36] Moghimi S M, Hunter A C and Murray J C 2001 *Pharmacological reviews* **53** 283–318
[37] Gizzatov A, Key J, Aryal S, Ananta J, Cervadoro A, Palange A L, Fasano M, Stigliano C, Zhong M, Di Mascolo D *et al.* 2014 *Advanced Functional Materials* **24** 4584–4594
[38] Brigger I, Dubernet C and Couvreur P 2002 *Advanced drug delivery reviews* **54** 631–651
[39] Liangruksa M, Ganguly R and Puri I 2011 *Journal of Magnetism and Magnetic Materials* **323** 708–716
[40] Cervadoro A, Cho M, Key J, Cooper C, Stigliano C, Aryal S, Brazdeikis A, Leary J F and Decuzzi P 2014 *ACS applied materials & interfaces* **6** 12939–12946
[41] Ruta S, Chantrell R and Hovorka O 2015 *Scientific reports* **5**
[42] Gupta A K and Gupta M 2005 *Biomaterials* **26** 3995–4021
[43] Keblinski P, Phillpot S, Choi S and Eastman J 2002 *International journal of heat and mass transfer* **45** 855–863
[44] Wang X Q and Mujumdar A S 2007 *International journal of thermal sciences* **46** 1–19
[45] Wen D, Lin G, Vafaei S and Zhang K 2009 *Particuology* **7** 141–150
[46] Khanafer K and Vafai K 2011 *International Journal of Heat and Mass Transfer* **54** 4410–4428
[47] Thomas S and Sobhan C B P 2011 *Nanoscale research letters* **6** 1–21
[48] Solangi K, Kazi S, Luhur M, Badarudin A, Amiri A, Sadri R, Zubir M, Gharehkhani S and Teng K 2015 *Energy* **89** 1065–1086
[49] Murshed S, Leong K and Yang C 2005 *International Journal of Thermal Sciences* **44** 367–373
[50] Li Y, Tung S, Schneider E, Xi S *et al.* 2009 *Powder Technology* **196** 89–101
[51] Angayarkanni S and Philip J 2015 *Advances in colloid and interface science* **225** 146–176
[52] Chandrasekar M, Suresh S and Bose A C 2010 *Experimental Thermal and Fluid Science* **34** 122 – 130
[53] Lomascolo M, Colangelo G, Milanese M and de Risi A 2015 *Renewable and Sustainable Energy Reviews* **43** 1182–1198
[54] Kole M and Dey T 2010 *Journal of Physics D: Applied Physics* **43** 315501
[55] Corcione M, Cianfrini M and Quintino A 2013 *Applied Thermal Engineering* **50** 857 – 867
[56] Hussein A M, Bakar R and Kadirgama K 2014 *Case Studies in Thermal Engineering* **2** 50 – 61
[57] Ray D R and Das D K 2014 *Journal of Thermal Science and Engineering Applications* **6** 041002

[58] Sidik N A C, Yazid M N A W M and Mamat R 2015 *International Communications in Heat and Mass Transfer* **68** 85–90

[59] Rashmi W, Khalid M, Ong S and Saidur R 2014 *Materials Research Express* **1** 032001

[60] Truzzolillo D, Roger V, Dupas C, Mora S and Cipelletti L 2015 *Journal of Physics: Condensed Matter* **27** 194103

[61] Arthur O and Karim M 2016 *Renewable and Sustainable Energy Reviews* **55** 739 – 755

[62] Azmi W, Sharma K, Mamat R, Najafi G and Mohamad M 2016 *Renewable and Sustainable Energy Reviews* **53** 1046–1058

[63] Keblinski P, Prasher R and Eapen J 2008 *Journal of Nanoparticle research* **10** 1089–1097

[64] Pop E, Mann D, Wang Q, Goodson K and Dai H 2006 *Nano Letters* **6** 96–100

[65] Sobhan C B and Peterson G P 2008 *Microscale and nanoscale heat transfer: fundamentals and engineering applications* (CRC Press)

[66] Cahill D G, Ford W K, Goodson K E, Mahan G D, Majumdar A, Maris H J, Merlin R and Phillpot S R 2002 *Journal of Applied Physics* **93** 793–818

[67] Bresme F and Oettel M 2007 *Journal of Physics: Condensed Matter* **19** 413101

[68] Lervik A, Bresme F and Kjelstrup S 2009 *Soft Matter* **5** 2407–2414

[69] Hu M, Goicochea J V, Michel B and Poulikakos D 2009 *Nano letters* **10** 279–285

[70] Chen Y and Zhang C 2014 *International Journal of Heat and Mass Transfer* **78** 624–629

[71] Barisik M and Beskok A 2014 *International Journal of Thermal Sciences* **77** 47–54

[72] Fasano M, Bigdeli M B, Sereshk M R V, Chiavazzo E and Asinari P 2015 *Renewable and Sustainable Energy Reviews* **41** 1028–1036

[73] Prasher R, Phelan P E and Bhattacharya P 2006 *Nano Letters* **6** 1529–1534

[74] Gao J, Zheng R, Ohtani H, Zhu D and Chen G 2009 *Nano letters* **9** 4128–4132

[75] Zheng R, Gao J, Wang J, Feng S P, Ohtani H, Wang J and Chen G 2011 *Nano letters* **12** 188–192

[76] Buongiorno J, Venerus D C, Prabhat N, McKrell T, Townsend J, Christianson R, Tolmachev Y V, Keblinski P, Hu L w, Alvarado J L *et al.* 2009 *Journal of Applied Physics* **106** 094312

[77] Hens A, Agarwal R and Biswas G 2014 *International Journal of Heat and Mass Transfer* **71** 303–312

[78] Mao Y and Zhang Y 2014 *Applied Thermal Engineering* **62** 607–612

[79] Fan J and Wang L 2010 *Journal of Physics D: Applied Physics* **43** 165501

[80] Tzou D 2008 *International Journal of Heat and Mass Transfer* **51** 2967–2979

[81] Piazza R and Parola A 2008 *Journal of Physics: Condensed Matter* **20** 153102

[82] Lüsebrink D, Yang M and Ripoll M 2012 *Journal of Physics: Condensed Matter* **24** 284132

[83] Eslamian M and Saghir M Z 2014 *International Journal of Thermal Sciences* **80** 58–64

[84] Etheridge M L, Campbell S A, Erdman A G, Haynes C L, Wolf S M and McCullough J 2013 *Nanomedicine: nanotechnology, biology and medicine* **9** 1–14

[85] Shih C J, Lin S, Strano M S and Blankschtein D 2015 *The Journal of Physical Chemistry C* **119** 1047–1060

[86] Das S, Choi S, Yu W and Pradeep T 2007 *Nanofluids: Science and Technology* (Wiley)

[87] Krajnik P, Pusavec F and Rashid A 2011 Nanofluids: Properties, applications and sustainability aspects in materials processing technologies *Advances in Sustainable Manufacturing* (Springer) pp 107–113

[88] Ma K Q and Liu J 2007 *Physics Letters A* **361** 252–256

[89] Zhang Q and Liu J 2013 *Nano Energy* **2** 863–872

[90] Wei X, Zhu H, Kong T and Wang L 2009 *International Journal of Heat and Mass Transfer* **52** 4371–4374

[91] Kim D, Kwon Y, Cho Y, Li C, Cheong S, Hwang Y, Lee J, Hong D and Moon S 2009 *Current Applied Physics* **9** e119–e123

[92] Munkhbayar B, Tanshen M R, Jeoun J, Chung H and Jeong H 2013 *Ceramics International* **39** 6415–6425

[93] Singh A K and Raykar V S 2008 *Colloid and Polymer Science* **286** 1667–1673

[94] De Robertis E, Cosme E, Neves R, Kuznetsov A Y, Campos A, Landi S and Achete C 2012 *Applied Thermal Engineering* **41** 10–17

[95] Bönnemann H, Botha S, Bladergroen B and Linkov V 2005 *Applied organometallic chemistry* **19** 768–773

[96] Mahbubul I, Saidur R and Amalina M 2012 *International Journal of Heat and Mass Transfer* **55** 874 – 885

[97] Garg P, Alvarado J L, Marsh C, Carlson T A, Kessler D A and Annamalai K 2009 *International Journal of Heat and Mass Transfer* **52** 5090–5101

[98] Meibodi M E, Vafaie-Sefti M, Rashidi A M, Amrollahi A, Tabasi M and Kalal H S 2010 *International Communications in Heat and Mass Transfer* **37** 319–323

[99] Lee D 2007 *Langmuir* **23** 6011–6018

[100] Kurt H and Kayfeci M 2009 *Applied Energy* **86** 2244–2248

[101] Wang X, Xu X and S Choi S U 1999 *Journal of thermophysics and heat transfer* **13** 474–480

[102] Pang C, Jung J Y, Lee J W and Kang Y T 2012 *International Journal of Heat and Mass Transfer* **55** 5597–5602

[103] Das S K, Putra N, Thiesen P and Roetzel W 2003 *Journal of Heat Transfer* **125** 567–574

[104] Wang X j, Zhu D s *et al.* 2009 *Chemical Physics Letters* **470** 107–111

[105] Oh D W, Jain A, Eaton J K, Goodson K E and Lee J S 2008 *International Journal of Heat and Fluid Flow* **29** 1456–1461

[106] Paul G, Chopkar M, Manna I and Das P 2010 *Renewable and Sustainable Energy Reviews* **14** 1913–1924

[107] Pantzali M, Kanaris A, Antoniadis K, Mouza A and Paras S 2009 *International Journal of Heat and Fluid Flow* **30** 691–699

[108] Starace A K, Gomez J C, Wang J, Pradhan S and Glatzmaier G C 2011 *Journal of Applied Physics* **110** 124323

[109] Elias M, Mahbubul I, Saidur R, Sohel M, Shahrul I, Khaleduzzaman S and Sadeghipour S 2014 *International Communications in Heat and Mass Transfer* **54** 48–53

[110] Nguyen C, Desgranges F, Roy G, Galanis N, Mar T, Boucher S and Angue Mintsa H 2007 *International Journal of Heat and Fluid Flow* **28** 1492–1506

[111] Xian-Ju W and Xin-Fang L 2009 *Chinese Physics Letters* **26** 056601

[112] Chandrasekar M, Suresh S and Chandra Bose A 2010 *Experimental Thermal and Fluid Science* **34** 210–216

[113] Vajjha R, Das D and Mahagaonkar B 2009 *Petroleum Science and Technology* **27** 612–624

[114] Mahian O, Kianifar A and Wongwises S 2013 *Journal of Cluster Science* **24** 1103–1114

[115] Eastman J, Choi S, Li S, Yu W and Thompson L 2001 *Applied Physics Letters* **78** 718–720

[116] Masuda H, Ebata A and Teramae K 1993 *Netsu Bussei*

[117] Beck M P, Yuan Y, Warrier P and Teja A S 2009 *Journal of Nanoparticle Research* **11** 1129–1136

[118] Lee W H, Rhee C K, Koo J, Lee J, Jang S P, Choi S U, Lee K W, Bae H Y, Lee G J, Kim C K *et al.* 2011 *Nanoscale research letters* **6** 1–11

[119] Zhang X, Gu H and Fujii M 2007 *Experimental Thermal and Fluid Science* **31** 593–599

[120] Pang C, Lee J W, Hong H and Kang Y T 2014 *Journal of Mechanical Science and Technology* **28** 2925–2936

[121] Bahiraei M and Hangi M 2015 *Journal of Magnetism and Magnetic Materials* **374** 125–138

[122] Hong T K, Yang H S and Choi C 2005 *Journal of Applied Physics* **97** 064311

[123] Vajjha R S and Das D K 2009 *International Journal of Heat and Mass Transfer* **52** 4675–4682

[124] Mintsa H A, Roy G, Nguyen C T and Doucet D 2009 *International Journal of Thermal Sciences* **48** 363–371

[125] Beck M P, Yuan Y, Warrier P and Teja A S 2010 *Journal of Nanoparticle research* **12** 1469–1477

[126] Xie H q, Wang J c, Xi T g and Liu Y 2002 *International Journal of Thermophysics* **23** 571–580

[127] Lee K J, Yoon S H and Jang J 2007 *Small* **3** 1209–1213

[128] Timofeeva E V, Routbort J L and Singh D 2009 *Journal of Applied Physics* **106** 014304

[129] Wensel J, Wright B, Thomas D, Douglas W, Mannhalter B, Cross W, Hong H, Kellar J, Smith P and Roy W 2008 *Applied Physics Letters* **92** 023110

[130] Xuan Y, Huang Y and Li Q 2009 *Chemical Physics Letters* **479** 264–269

[131] Jana S, Salehi-Khojin A and Zhong W H 2007 *Thermochimica acta* **462** 45–55

[132] Kim Y J, Ma H and Yu Q 2010 *Nanotechnology* **21** 295703

[133] Xuan Y, Li Q and Hu W 2003 *AIChE Journal* **49** 1038–1043

[134] Xie H, Wang J, Xi T, Liu Y, Ai F and Wu Q 2002 *Journal of Applied Physics* **91** 4568–4572

[135] Assael M, Metaxa I, Arvanitidis J, Christofilos D and Lioutas C 2005 *International Journal of Thermophysics* **26** 647–664

[136] Habibzadeh S, Kazemi-Beydokhti A, Khodadadi A A, Mortazavi Y, Omanovic S and Shariat-Niassar M 2010 *Chemical Engineering Journal* **156** 471 – 478

[137] Angayarkanni S and Philip J 2013 *The Journal of Physical Chemistry C* **117** 9009–9019

[138] Li C H, Williams W, Buongiorno J, Hu L W and Peterson G 2008 *Journal of Heat Transfer* **130** 042407

[139] Das S K, Putra N and Roetzel W 2003 *International Journal of Heat and Mass Transfer* **46** 851–862

[140] Buongiorno J 2006 *Journal of Heat Transfer* **128** 240–250

[141] Lai W, Vinod S, Phelan P and Prasher R 2009 *Journal of Heat Transfer* **131** 112401

[142] Said Z, Sajid M, Saidur R, Kamalisarvestani M and Rahim N 2013 *International Communications in Heat and Mass Transfer* **46** 74–84

[143] Zhu Q, Cui Y, Mu L and Tang L 2013 *International Journal of Thermophysics* **34** 2307–2321

[144] Kim H D, Kim J and Kim M H 2007 *International journal of multiphase flow* **33** 691–706

[145] Kim S J, McKrell T, Buongiorno J and Hu L W 2009 *Journal of Heat Transfer* **131** 043204

[146] You S, Kim J and Kim K 2003 *Applied Physics Letters* **83** 3374–3376

[147] Wen D and Ding Y 2005 *Journal of Nanoparticle Research* **7** 265–274

[148] Liu Z h, Xiong J g and Bao R 2007 *International Journal of Multiphase Flow* **33** 1284–1295

[149] Bang I C and Chang S H 2005 *International Journal of Heat and Mass Transfer* **48** 2407–2419

[150] Zhou S Q and Ni R 2008 *Applied Physics Letters* **92** 093123–093123

[151] Vajjha R S and Das D K 2009 *Journal of heat transfer* **131** 071601

[152] Wang B X, Zhou L P and Peng X F 2006 *International journal of thermophysics* **27** 139–151

[153] Nayak A, Singh R and Kulkarni P 2009 *Applied Physics Letters* **94** 094102

[154] Nayak A, Singh R and Kulkarni P 2010 *Technical Physics Letters* **36** 696–698

[155] Shaikh S, Lafdi K and Hallinan K 2008 *Journal of applied physics* **103** 094302

[156] Harikrishnan S and Kalaiselvam S 2012 *Thermochimica Acta* **533** 46–55

[157] Mena J B, Ubices de Moraes A A, Benito Y R, Ribatski G and Parise J A R 2013 *Applied Thermal Engineering* **51** 1092–1097

[158] Heine D R, Petersen M K and Grest G S 2010 *The Journal of Chemical Physics* **132** 184509

[159] Wamkam C T, Opoku M K, Hong H and Smith P 2011 *Journal of Applied Physics* **109** 024305

[160] Kim S, Kim C, Lee W H and Park S R 2011 *Journal of Applied Physics* **110** 034316

[161] Phuoc T X, Massoudi M and Chen R H 2011 *International Journal of Thermal Sciences* **50** 12–18

[162] Kamranfar P and Jamialahmadi M 2014 *Journal of Molecular Liquids*

[163] He Y, Jin Y, Chen H, Ding Y, Cang D and Lu H 2007 *International Journal of Heat and Mass Transfer* **50** 2272–2281

[164] Nguyen C, Desgranges F, Galanis N, Roy G, Maré T, Boucher S and Angue Mintsa H 2008 *International Journal of Thermal Sciences* **47** 103–111

[165] Sahoo B C, Vajjha R S, Ganguli R, Chukwu G A and Das D K 2009 *Petroleum Science and Technology* **27** 1757–1770

[166] Yu W, Xie H, Li Y and Chen L 2011 *Particuology* **9** 187 – 191

[167] Ghanbarpour M, Bitaraf Haghigi E and Khodabandeh R 2014 *Experimental Thermal and Fluid Science* **53** 227–235

[168] Murshed S S, Tan S H and Nguyen N T 2008 *Journal of Physics D: Applied Physics* **41** 085502

[169] Choy T C 2015 *Effective medium theory: principles and applications* (Oxford University Press)

[170] Yu W and Choi S 2003 *Journal of Nanoparticle Research* **5** 167–171

[171] Feng Y, Yu B, Xu P and Zou M 2007 *Journal of Physics D: Applied Physics* **40** 3164

[172] Evans W, Prasher R, Fish J, Meakin P, Phelan P and Keblinski P 2008 *International Journal of Heat and Mass Transfer* **51** 1431–1438

[173] Warzoha R J and Fleischer A S 2014 *Nano Energy* **6** 137–158

[174] Jang S P and Choi S U 2004 *Applied physics letters* **84** 4316–4318

[175] Koo J and Kleinstreuer C 2004 *Journal of Nanoparticle Research* **6** 577–588

[176] Kumar D H, Patel H E, Kumar V R, Sundararajan T, Pradeep T and Das S K 2004 *Physical Review Letters* **93** 144301

[177] Prasher R, Bhattacharya P and Phelan P E 2005 *Physical Review Letters* **94** 025901

[178] Evans W, Fish J and Keblinski P 2006 *Applied Physics Letters* **88** 093116

[179] Patel H E, Sundararajan T and Das S K 2008 *Journal of Nanoparticle Research* **10** 87–97

[180] Özerinç S, Kakaç S and Yazıcıoğlu A G 2010 *Microfluidics and Nanofluidics* **8** 145–170

[181] Kleinstreuer C and Feng Y 2011 *Nanoscale research letters* **6** 1–13

[182] Maxwell J C 1873 *A treatise on electricity and magnetism* vol 1 (Clarendon press)

[183] Hamilton R and Crosser O 1962 *Industrial & Engineering chemistry fundamentals* **1** 187–191

[184] Murshed S, Leong K and Yang C 2009 *Applied Thermal Engineering* **29** 2477–2483

[185] Hasselman D and Johnson L F 1987 *Journal of Composite Materials* **21** 508–515

[186] Wang B X, Zhou L P and Peng X F 2003 *International Journal of Heat and Mass Transfer* **46** 2665–2672

[187] Corcione M 2011 *Energy Conversion and Management* **52** 789–793

[188] Chon C H, Kihm K D, Lee S P and Choi S U 2005 *Applied Physics Letters* **87** 153107–153107

[189] Pak B C and Cho Y I 1998 *Experimental Heat Transfer: A Journal of Thermal Energy Generation, Transport, Storage, and Conversion* **11** 151–170

[190] Gosselin L and da Silva A K 2004 *Applied Physics Letters* **85** 4160–4162

[191] O'Hanley H, Buongiorno J, McKrell T and Hu L w 2012 *Advances in Mechanical Engineering* **2012**

[192] Murshed S S 2012 *Heat Transfer Engineering* **33** 722–731

[193] Murshed S S 2011 *Journal of Experimental Nanoscience* **6** 539–546

[194] Xuan Y and Roetzel W 2000 *International Journal of Heat and Mass Transfer* **43** 3701–3707

[195] Ho C, Liu W, Chang Y and Lin C 2010 *International Journal of Thermal Sciences* **49** 1345–1353

[196] Mansour R B, Galanis N and Nguyen C T 2007 *Applied Thermal Engineering* **27** 240 – 249

[197] Namburu P, Kulkarni D, Dandekar A and Das D 2007 *Micro & Nano Letters, IET* **2** 67–71

[198] Khanafer K, Vafai K and Lightstone M 2003 *International Journal of Heat and Mass Transfer* **46** 3639–3653

[199] Ho C J, Chen M and Li Z 2008 *International Journal of Heat and Mass Transfer* **51** 4506–4516

[200] Einstein A 1906 *Annalen der Physik* **324** 289–306

[201] Brinkman H C 1952 *The Journal of Chemical Physics* **20** 571–571

[202] Lundgren T S 1972 *Journal of Fluid Mechanics* **51** 273–299

[203] Batchelor G 1977 *Journal of Fluid Mechanics* **83** 97–117

[204] Graham A L 1981 *Applied Scientific Research* **37** 275–286

[205] Krieger I M and Dougherty T J 1959 *Transactions of the Society of Rheology* **3** 137–152

[206] Chen H, Ding Y, He Y and Tan C 2007 *Chemical Physics Letters* **444** 333–337

[207] Longo G A, Zilio C, Ceseracciu E and Reggiani M 2012 *Nano Energy* **1** 290–296

[208] Tseng W J and Lin K C 2003 *Materials Science and Engineering: A* **355** 186 – 192

[209] Palm S J, Roy G and Nguyen C T 2006 *Applied Thermal Engineering* **26** 2209 – 2218

[210] Kulkarni D P, Das D K and Vajjha R S 2009 *Applied Energy* **86** 2566 – 2573

[211] Pastoriza-Gallego M, Casanova C, Legido J and Pieiro M 2011 *Fluid Phase Equilibria* **300** 188 – 196

[212] Puliti G, Paolucci S and Sen M 2011 *Journal of Nanoparticle Research* **13** 4277–4293

[213] Chiavazzo E, Fasano M, Asinari P and Decuzzi P 2014 *Nature communications* **5**

[214] Gerardi C, Cory D, Buongiorno J, Hu L W and McKrell T 2009 *Applied Physics Letters* **95** 253104

[215] Chen L and Xie H 2010 *Thermochimica Acta* **497** 67–71

[216] Choi C, Yoo H and Oh J 2008 *Current Applied Physics* **8** 710–712

[217] Fasano M, Chiavazzo E and Asinari P 2014 *Nanoscale research letters* **9** 1–8

[218] Turanov A and Tolmachev Y V 2009 *Heat and mass transfer* **45** 1583–1588

[219] Khan S H, Matei G, Patil S and Hoffmann P M 2010 *Physical review letters* **105** 106101

[220] Riedo E *et al.* 2008 *Physical review letters* **100** 106102

[221] Goertz M P, Houston J and Zhu X Y 2007 *Langmuir* **23** 5491–5497

[222] Chen S H, Mallamace F, Mou C Y, Broccio M, Corsaro C, Faraone A and Liu L 2006 *Proceedings of the National Academy of Sciences* **103** 12974–12978

[223] Tankeshwar K and Srivastava S 2007 *Nanotechnology* **18** 485714

[224] Mazza M G, Giovambattista N, Stanley H E and Starr F W 2007 *Physical Review E* **76** 031203

[225] Xu L, Mallamace F, Yan Z, Starr F W, Buldyrev S V and Stanley H E 2009 *Nature Physics* **5** 565–569

[226] Hong K and Noolandi J 1978 *The Journal of Chemical Physics* **68** 5163–5171

[227] Wilemski G 1976 *Journal of Statistical Physics* **14** 153–169

[228] Swift D L and Friedlander S 1964 *Journal of colloid science* **19** 621–647

[229] Friedlander S and Wang C 1966 *Journal of Colloid and interface Science* **22** 126–132

[230] Derjaguin B and Landau L 1941 *Acta Physicochim. URSS* **14** 633–52

[231] Verwey E and Overbeek J T G 1955 *Journal of Colloid Science* **10** 224–225

[232] Hunter R J 2001 *Foundations of colloid science* (Oxford University Press Inc.)

[233] Hamaker H 1937 *physica* **4** 1058–1072

[234] Trefalt G 2012 *A New Synthesis Route to Pb (Mg$_{1/3}$Nb$_{2/3}$)O$_3$–based Materials by the Controlled Agglomeration of Reagent Particles: Doctoral Dissertation* Ph.D. thesis G. Trefalt

[235] Lee D, Kim J W and Kim B G 2006 *The Journal of Physical Chemistry B* **110** 4323–4328

[236] Kulshreshtha A K, Singh O N and Wall G M 2009 *Pharmaceutical suspensions: from formulation development to manufacturing* (Springer)

[237] White S B, Shih A J M and Pipe K P 2011 *Nanoscale research letters* **6** 1–5

[238] Li X, Zhu D, Wang X, Wang N, Gao J and Li H 2008 *Thermochimica Acta* **469** 98–103

[239] Tadros T F 2006 *Applied surfactants: principles and applications* (John Wiley & Sons)

[240] Wen D, Lin G, Vafaei S and Zhang K 2009 *Particuology* **7** 141–150

[241] Wong J Y, Kuhl T L, Israelachvili J N, Mullah N and Zalipsky S 1997 *Science* **275** 820–822

[242] Lin S, Shih C J, Strano M S and Blankschtein D 2011 *Journal of the American Chemical Society* **133** 12810–12823

[243] Pashley R 1981 *Journal of Colloid and Interface Science* **83** 531–546

[244] Israelachvili J N and Pashley R M 1983 *Nature* **306** 249–250

[245] Shih C J, Lin S, Strano M S and Blankschtein D 2010 *Journal of the American Chemical Society* **132** 14638–14648

[246] Pastoriza-Gallego M, Casanova C, Páramo R, Barbés B, Legido J and Piñeiro M 2009 *Journal of Applied Physics* **106** 064301

[247] Swartz E T and Pohl R O 1989 *Reviews of Modern Physics* **61** 605

[248] Li J and Kleinstreuer C 2008 *International Journal of Heat and Fluid Flow* **29** 1221–1232

[249] Timofeeva E V, Smith D S, Yu W, France D M, Singh D and Routbort J L 2010 *Nanotechnology* **21** 215703

[250] Stevens R J, Zhigilei L V and Norris P M 2007 *International Journal of Heat and Mass Transfer* **50** 3977–3989

[251] Ge Z, Cahill D G and Braun P V 2006 *Physical review letters* **96** 186101

[252] Hu L, Desai T and Keblinski P 2011 *Physical Review B* **83** 195423

[253] Putnam S A, Cahill D G, Ash B J and Schadler L S 2003 *Journal of applied physics* **94** 6785–6788

[254] Jiang H, Li H, Xu Q and Shi L 2014 *Materials Chemistry and Physics* **148** 195–200

[255] Yu W and Choi S 2004 *Journal of Nanoparticle Research* **6** 355–361

[256] Xue Q and Xu W M 2005 *Materials Chemistry and Physics* **90** 298–301

[257] Li L, Zhang Y, Ma H and Yang M 2010 *Journal of nanoparticle research* **12** 811–821

[258] Jang S P and Choi S U 2004 *Applied physics letters* **84** 4316–4318

[259] Bhattacharya P, Saha S, Yadav A, Phelan P and Prasher R 2004 *Journal of Applied Physics* **95** 6492–6494

[260] Einstein A 1956 *Investigations on the Theory of the Brownian Movement* (Courier Dover Publications)

[261] Babaei H, Keblinski P and Khodadadi J 2013 *Journal of Applied Physics* **113** 084302

[262] Russel W B, Saville D A and Schowalter W R 1992 *Colloidal dispersions* (Cambridge university press)

[263] Chen H, Ding Y and Tan C 2007 *New journal of physics* **9** 367

[264] Duan F, Kwek D and Crivoi A 2011 *Nanoscale research letters* **6** 1–5

[265] Wu C, Cho T J, Xu J, Lee D, Yang B and Zachariah M R 2010 *Physical Review E* **81** 011406

[266] Weitz D, Huang J, Lin M and Sung J 1985 *Physical review letters* **54** 1416

[267] Philip J, Shima P and Raj B 2008 *Nanotechnology* **19** 305706

[268] Shima P, Philip J and Raj B 2009 *Applied Physics Letters* **94** 223101

[269] Sattler K D 2010 *Handbook of Nanophysics: Nanoparticles and Quantum Dots* (CRC press)

[270] Carson J K, Lovatt S J, Tanner D J and Cleland A C 2005 *International Journal of Heat and Mass Transfer* **48** 2150 – 2158

[271] Nan C W, Birringer R, Clarke D R and Gleiter H 1997 *Journal of Applied Physics* **81** 6692–6699

[272] Eapen J, Rusconi R, Piazza R and Yip S 2010 *Journal of heat transfer* **132** 102402

[273] Dhar P, Gupta S S, Chakraborty S, Pattamatta A and Das S K 2013 *Applied Physics Letters* **102** 163114

[274] Mercatelli L, Sani E, Fontani D, Zaccanti G, Martelli F and Di Ninni P 2011 *Journal of the European Optical Society-Rapid publications* **6**

[275] Xie T, He Y L and Hu Z J 2013 *International Journal of Heat and Mass Transfer* **58** 540–552

[276] Otanicar T P, Phelan P E, Prasher R S, Rosengarten G and Taylor R A 2010 *Journal of renewable and sustainable energy* **2** 033102

[277] Otanicar T P, Phelan P E and Golden J S 2009 *Solar Energy* **83** 969–977

[278] Otanicar T P, Theisen S, Norman T, Tyagi H and Taylor R A 2015 *Applied Energy* **140** 224–233

[279] Bohren C F and Huffman D R 2008 *Absorption and scattering of light by small particles* (John Wiley & Sons)

[280] Sani E, Mercatelli L, Barison S, Pagura C, Agresti F, Colla L and Sansoni P 2011 *Solar Energy Materials and Solar Cells* **95** 2994–3000

[281] Sani E, Barison S, Pagura C, Mercatelli L, Sansoni P, Fontani D, Jafrancesco D and Francini F 2010 *Optics Express* **18** 5179–5187

[282] Young D A and Maris H J 1989 *Phys. Rev. B* **40**(6) 3685–3693

[283] Schelling P K, Phillpot S R and Keblinski P 2002 *Physical Review B* **65** 144306

[284] Zhang W, Fisher T and Mingo N 2007 *Journal of heat transfer* **129** 483–491

[285] Vladkov M and Barrat J L 2006 *Nano letters* **6** 1224–1228

[286] Zhou X W, Jones R E, Kimmer C J, Duda J C and Hopkins P E 2013 *Physical Review B* **87** 094303

[287] Chen X, Munjiza A, Zhang K and Wen D 2014 *The Journal of Physical Chemistry C* **118** 1285–1293

[288] Eapen J, Li J and Yip S 2007 *Physical Review E* **76** 062501

[289] Lee S, Saidur R, Sabri M and Min T 2015 *Numerical Heat Transfer, Part A: Applications* **68** 432–453

[290] Shenogina N, Godawat R, Keblinski P and Garde S 2009 *Physical review letters* **102** 156101

[291] Desai T G 2011 *Applied Physics Letters* **98** 193107

[292] Calzolari A, Jayasekera T, Kim K W and Nardelli M B 2012 *Journal of Physics: Condensed Matter* **24** 492204

[293] Stewart D A, Savic I and Mingo N 2008 *Nano letters* **9** 81–84

[294] Zhang L, Zahid F, Zhu Y, Liu L, Wang J, Guo H, Chan P C and Chan M 2013 *Electron Devices, IEEE Transactions on* **60** 3527–3533

[295] Mingo N and Yang L 2003 *Physical Review B* **68** 245406

[296] Walczak K and Yerkes K L 2014 *Journal of Applied Physics* **115** 174308

[297] Ong Z Y and Zhang G 2015 *Physical Review B* **91** 174302

[298] Mingo N 2009 Green's function methods for phonon transport through nano-contacts *Thermal nanosystems and nanomaterials* (Springer) pp 63–94

[299] Bolintineanu D S, Grest G S, Lechman J B, Pierce F, Plimpton S J and Schunk P R 2014 *Computational Particle Mechanics* **1** 321–356

[300] Dunweg B and Ladd A J 2008 *Advanced Computer Simulation Approaches for Soft Matter Sciences III* **221** 89

[301] Ladd A and Verberg R 2001 *Journal of Statistical Physics* **104** 1191–1251

[302] Chen S and Doolen G D 1998 *Annual review of fluid mechanics* **30** 329–364

[303] Asinari P 2006 *Physical Review E* **73** 056705

[304] Fujita M and Yamaguchi Y 2008 *Physical Review E* **77** 026706

[305] Delong S, Usabiaga F B, Delgado-Buscalioni R, Griffith B E and Donev A 2014 *The Journal of chemical physics* **140** 134110

[306] Keaveny E E 2014 *Journal of Computational Physics* **269** 61–79

[307] Gompper G, Ihle T, Kroll D and Winkler R 2009 Multi-particle collision dynamics: a particle-based mesoscale simulation approach to the hydrodynamics of complex fluids *Advanced computer simulation approaches for soft matter sciences III* (Springer) pp 1–87

[308] Padding J and Louis A 2006 *Physical Review E* **74** 031402

[309] Malevanets A and Kapral R 1999 *The Journal of chemical physics* **110** 8605–8613

[310] Laganapan A M, Mouas M, Videcoq A, Cerbelaud M, Bienia M, Bowen P and Ferrando R 2015 *Journal of colloid and interface science* **458** 241–246

[311] Espanol P 1995 *Physical Review E* **52** 1734

[312] Espanol P and Warren P 1995 *EPL (Europhysics Letters)* **30** 191

[313] Hoogerbrugge P and Koelman J 1992 *EPL (Europhysics Letters)* **19** 155

[314] Kumar A and Higdon J J 2010 *Physical Review E* **82** 051401

[315] Brady J F and Bossis G 1988 *Annual review of fluid mechanics* **20** 111–157

[316] Liu H H, Surawanvijit S, Rallo R, Orkoulas G and Cohen Y 2011 *Environmental science & technology* **45** 9284–9292

[317] Liu H H, Lanphere J, Walker S and Cohen Y 2015 *Nanotechnology* **26** 045708

[318] Mortuza S, Kariyawasam L K and Banerjee S 2015 *Physical Review E* **92** 013304

[319] Chiavazzo E and Asinari P 2010 *International Journal of Thermal Sciences* **49** 2272–2281

[320] Gharagozloo P E and Goodson K E 2010 *Journal of Applied Physics* **108** 074309

[321] Gharagozloo P E and Goodson K E 2011 *International Journal of Heat and Mass Transfer* **54** 797–806

[322] Sastry N V, Bhunia A, Sundararajan T and Das S K 2008 *Nanotechnology* **19** 055704

[323] Lamas B, Abreu B, Fonseca A, Martins N and Oliveira M 2013 *International Journal for Numerical Methods in Engineering* **95** 257–270